HHS Public Access

Author manuscript

Immunity. Author manuscript; available in PMC 2022 January 12.

Published in final edited form as:

Immunity. 2021 January 12; 54(1): 151–163.e6. doi:10.1016/j.immuni.2020.10.014.

Interleukin-33 promotes serotonin release from enterochromaffin cells for intestinal homeostasis

Zuojia Chen[1,9], **Jialie Luo**[1,9], **Jian Li**[1], **Girak Kim**[1], **Andy Stewart**[2], **Joseph F. Urban Jr.**[3], **Yuefeng Huang**[4,5], **Shan Chen**[6], **Ling-Gang Wu**[7], **Alexander Chesler**[8], **Giorgio Trinchieri**[2], **Wei Li**[6], **Chuan Wu**[1,10]

[1]Experimental Immunology Branch, National Cancer Institute, NIH, Bethesda, MD, USA;

[2]Cancer and Inflammation Program, Center for Cancer Research, National Cancer Institute, NIH, Bethesda, MD, USA;

[3]U.S. Department of Agriculture, Agricultural Research Service, Beltsville Human Nutrition Research Center, Diet, Genomics, and Immunology Laboratory, Beltsville, MD, USA;

[4]Laboratory of Immunology, National Institute of Allergy and Infectious Diseases, NIH, Bethesda, MD, USA;

[5]Present addresses: Department of Microbiology and Immunology, Columbia University, NY, USA;

[6]Retinal Neurophysiology Section, National Eye Institute, NIH, Bethesda, MD, USA;

[7]Synaptic Transmission Section, National Institute of Neurological Disorders and Stroke, NIH, Bethesda, MD, USA;

[8]Sensory Cells and Circuits Section, National Center for Complementary and Integrative Health, NIH, Bethesda, MD, USA;

[9]These authors contributed equally to this work

[10]Lead contact

Abstract

The gastrointestinal tract is known as the largest endocrine organ that encounters and integrates various immune stimulations and neuronal responses due to constant environmental challenges. Enterochromaffin (EC) cells which function as chemosensors on the gut epithelium are known to translate environmental cues into serotonin (5-HT) production, contributing to intestinal physiology. However, how immune signals participate in gut sensation and neuroendocrine

Correspondence: Chuan Wu (chuan.wu@nih.gov).

Authors' contribution

Planning and Conceptualization, Z.J. and C.W.; Experimentation and Data Analysis, Z.J., J.L., J.L., G.K., Y.H. and S.C.; Provision of Key Resources, A.S., J.F.U., L-G.W., A.C., G.T. and W.L.; Writing and Editing Manuscript, Z.C., J.L., and C.W., Supervision, C.W.

Declaration of Interests

The authors declare no competing interests.

response remains unclear. Interleukin-33 (IL-33) act as an alarmin cytokine by alerting the system of potential environmental stresses. We here demonstrate that IL-33 induced instantaneous peristaltic movement and facilitated *Trichuris muris* expulsion. We found that IL-33 could be sensed by EC cells, inducing release of 5-HT. IL-33-mediated 5-HT release activated enteric neurons, subsequently promoting gut motility. Mechanistically, IL-33 triggered calcium influx via a non-canonical signaling pathway specifically in EC cells to induce 5-HT secretion. Our data establish an immune-neuroendocrine axis in calibrating rapid 5-HT release for intestinal homeostasis.

Graphical Abstract

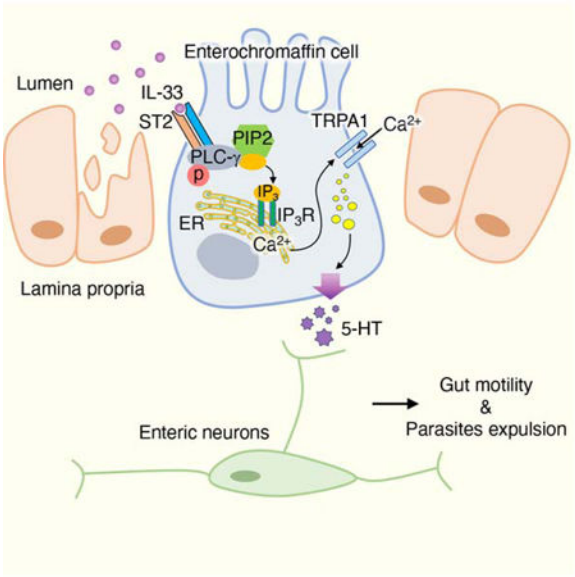

Abstract

Enterochromaffin (EC) cells are known to act as chemosensors on the gut epithelium, translating environmental cues into serotonin (5-HT) production. Chen et al demonstrate that an alarmin cytokine IL-33 could be sensed by EC cells, inducing release of 5-HT, regulating intestinal homeostasis and host defense.

Introduction

The intestinal epithelium is known to serve as an interface to exchange information between the external environment and host. Since the gut also functions as a major endocrine organ, the efficient conversion from environmental cues to host responses is critical for regulation of intestinal physiology. Coordination between the immune system and the neuroendocrine system is essential for environmental sensation and host defense (Furness et al., 2013). Abnormal immune regulation could lead to various intestinal neuroendocrine disorders (O'Malley et al., 2011; Rehn et al., 2004; Xia et al., 1999; Zhang et al., 2013). However, the underlying mechanisms of how immune-neuron crosstalk governs intestinal homeostasis require further investigation.

Interleukin-33 (IL-33), an IL-1 family member, acts as an alarmin cytokine in the gut, which is important for intestinal development and inflammation (Liew et al., 2016). IL-33 binds to its unique receptor, ST2, which is found on both hematopoietic and non-hematopoietic cells (Liew et al., 2016; Schmitz et al., 2005). The extensive external insults and rapid epithelial renewal lead to the abundance of IL-33 within the gut microenvironment even in a quiescent state (Creamer et al., 1961), suggesting a physiologic need of IL-33-mediated immune signaling for intestinal homeostasis. Moreover, IL-33 is recognized as a key cytokine in host defense as evidenced by worm infections by promoting type 2 immune response (Humphreys et al., 2008; Hung et al., 2013). However, since recent findings indicate that IL-33 plays critical roles in tissue repair (Burzyn et al., 2013; Gadani et al., 2015) and pain sensation (Han et al., 2013; Zarpelon et al., 2016), it is possible that IL-33 controls intestinal physiology and pathophysiology in a type 2 immunity-independent manner.

Enterochromaffin (EC) cells are one subset of specialized intestinal epithelial cells (IECs) that act as chemosensors to detect various environmental stimuli, including gut microbiota, mechanical stimulation and metabolites, leading to the generation and secretion of serotonin (5-hydroxytryptamine (5-HT)) (Bellono et al., 2017). In fact EC cells produce more than 90% of the peripheral 5-HT in the body (Gershon and Tack, 2007), which is crucial for intestinal peristalsis, platelet function, immune responses, bone development and cardiac function (Baganz and Blakely, 2013; Crane et al., 2015; Launay et al., 2002; Mercado et al., 2013; Yadav et al., 2010). As one key intestinal hormone, disrupted 5-HT results in various neurological and metabolic diseases, including irritable bowel syndrome (IBS) (Stasi et al., 2014). Thus, to illustrate how EC cells regulate 5-HT release is vital for understanding the maintenance of both intestinal and systemic homeostasis. Meanwhile, by harboring large quantities of microbiota and immune cells, the intestinal lumen is filled with a variety of immune regulators, such as antimicrobial peptides, proteinases, pattern recognition proteins, and cytokines. Despite emerging evidence that different sensory receptors have been identified in EC cells which detect specific environmental cues for 5-HT release (Alcaino et al., 2018; Bellono et al., 2017), it is still unclear whether and how immune signals participate in gut sensation by EC cells for intestinal physiologies and pathologies.

Here we identified a role of IL-33 in inducing instantaneous peristaltic movement, facilitating intestinal helminth clearance in a manner independent of type 2 immunity. Secretomics screening and *in situ* Ca^{2+} imaging revealed that IL-33-ST2 signaling specifically induced rapid release of 5-HT by EC cells to activate enteric neurons and promote gut motility. Loss of ST2 in EC cells resulted in impaired peripheral 5-HT release and parasite clearance without altering type 2 immune responses. Furthermore, ion channel screening and single EC cell electrophysiology studies uncovered that IL-33-mediated 5-HT release in EC cells was transient receptor potential ankyrin 1 (TRPA1)-dependent. Importantly, instead of canonical ST2-MyD88 signaling cascade, we demonstrate that IL-33 transduced a non-canonical signaling pathway to induce robust calcium influx specifically in EC cells, leading to rapid release of 5-HT in both murine and human EC cells. Hence, our data illustrate a gut sensation machinery in detecting immune signal for rapid neuroendocrinal responses to regulate intestinal homeostasis and host defense against enteric infection.

Results

IL-33 promotes *T. muris* expulsion in a type 2 immune response-independent manner.

We first asked whether IL-33-mediated parasite clearance occurs exclusively via type 2 immune responses. We infected *Il4*$^{-/-}$*Il13*$^{-/-}$ mice that lack type 2 responses, with the rodent colonic whipworm *Trichuris muris* (*T. muris*) (Antignano et al., 2011) Consistent with previous data (Antignano et al., 2011; Fallon et al., 2002), WT mice exhibited similar colonic goblet cell numbers under the naïve state but enhanced goblet cell hyperplasia during infection compared to *Il4*$^{-/-}$*Il13*$^{-/-}$ mice (Figure S1A–S1C). A kinetic study showed that *Il4*$^{-/-}$*Il13*$^{-/-}$ mice exhibited more *T. muris* clearance on day 21 than day 14, suggesting that in addition to type 2 responses, other regulatory mechanisms might be also involved in *T. muris* clearance (Figure S1D). Next, we observed that IL-33 administration elevated type 2 immune responses, leading to further elevated goblet cell hyperplasia in infected WT but not *Il4*$^{-/-}$*Il13*$^{-/-}$ mice (Figure 1A–1C). Despite the loss of type 2 cytokines in *Il4*$^{-/-}$*Il13*$^{-/-}$ mice, IL-33 treatment still promoted *T. muris* clearance without inducing goblet cell hyperplasia (Figure 1B–1D), suggesting that alternative mechanisms might be involved in IL-33-mediated *T. muris* clearance. In fact, it has been reported that intestinal peristaltic movement is critical for parasites expulsion (Vallance and Collins, 1998). Indeed, we found enhanced gut motility in IL-33-treated WT or *Il4*$^{-/-}$*Il13*$^{-/-}$ infected mice compared to control mice (Figure 1E). Furthermore, we validated these observations in a different genetic mouse strain of *Rag2*$^{-/-}$*Il2rg*$^{-/-}$ which lack innate and adaptive lymphocytes, including T helper-2 (Th2) cells and group 2 innate lymphoid cells (ILC2) (Figure S1E–S1H). Collectively, our data implicate that in addition to type 2 immune responses, IL-33 may facilitate *T. muris* clearance through enhancing intestinal peristalsis.

IL-33-ST2 signaling regulates gut motility.

In order to further verify the role of IL-33 in gut motility, we administered IL-33 to naïve WT mice for a week and found reduced colonic transit time compared to those treated with PBS (Figure 2A). Meanwhile, *Il33*$^{-/-}$ and *Il1rl1*$^{-/-}$ (*Il1rl1* encodes the IL-33 receptor, ST2.) mice both showed prolonged colonic transit time compared to controls (Figure 2B). Colonic tissues from *Il33*$^{-/-}$ and *Il1rl1*$^{-/-}$ mice exhibited compromised peristaltic contraction compared to those from WT mice (Figure 2C and 2D). And gut motility was found restored in *Il33*$^{-/-}$ but not *Il1rl1*$^{-/-}$ mice after a week of IL-33 treatment (Figure 2E). Additionally, given the abundance of bacteria within the intestine, we also examined and excluded the possibility that IL-33-mediated gut motility was due to gut microbiota (Figure S2A). We then asked whether IL-33 acutely regulated gut motility. We found that shortened colonic transit time after 10 minutes of IL-33 injection in a dose-dependent manner (Figure S2B and 2F). We confirmed that IL-33 induced rapid colonic tissue contraction in WT and *Il33*$^{-/-}$ mice but not *Il1rl1*$^{-/-}$ mice *in vitro* (Figure 2G). These results suggest that IL-33-ST2 signaling induces instantaneous peristaltic movement.

IEC-derived ST2 is required for gut motility.

Next, we attempted to determine which cells were responsible for IL-33-mediated gut motility. We found that T cells, ILCs, mast cells, intestinal macrophages and basophils did not respond to IL-33 to promote gut motility (Figure 3A). Given the rapid peristaltic

responses, we hypothesized that IL-33 might trigger a neuronal or muscular response. We then deleted ST2 on different enteric neurons, glia cells and smooth muscle cells, and found no impact on colonic transit time (Figure 3B). Lastly, it has been previously reported that ST2 on IECs is critical for intestinal homeostasis (Mahapatro et al., 2016). We then discovered that loss of ST2 in IECs markedly compromised colonic transit time (Figure 3C, S3A and S3B). Deletion of ST2 in IECs also abolished the rapid IL-33-induced colonic contractive response (Figure 3D and 3E).

Since enteric neurons are known to be critical for peristaltic movement (Furness, 2012), we asked whether IEC-mediated gut motility required enteric neuron activation. Consistent with previous studies (Gabanyi et al., 2016), we observed that enteric neurons innervate into the intestinal epithelium (Figure S3C). By whole mount intestinal tissue analysis from *Il33*^{GFP} reporter mice, we noticed that cells expressing IL-33 were close to, but not overlapping with enteric neurons (Figure S3C), excluding the intrinsic effect of IL-33 on these neurons. We then employed *Pirt*^{GCaMP3} mice which carry a calcium indicator in enteric neurons to reflect neuronal activities (Rakhilin et al., 2016). We treated isolated colonic tissue with IL-33 and observed enhanced neuronal activity in the myenteric plexus (Figure S3D, 3F and 3G). Removal of the epithelium layer abolished IL-33-mediated neuronal responses (Figure S3E, 3G and 3H), suggesting that IECs play a key role in mediating IL-33-induced gut motility by activating enteric neurons.

IL-33 induces 5-HT secretion for gut motility.

To address why IL-33-induced neuronal activation depends on IECs, we hypothesized that IL-33 might promote certain neurotransmitters or hormone secretion through specific IEC subpopulations which activate enteric neurons (Furness et al., 2013). Thus, we screened known IEC-derived secreted products in the serum after 10 minutes of IL-33 injection and found marked upregulation of 5-HT (Figure 4A). Indeed, kinetic studies showed robustly enhanced serum 5-HT after 10 minutes of IL-33 administration (Figure 4B), indicating that IL-33 promotes rapid 5-HT secretion. Consistently, we detected reduced serum 5-HT in *Il33*$^{-/-}$ and *Il1rl1*$^{-/-}$ mice compared to WT mice (Figure S4A).

Tryptophan hydroxylase 1 (Tph1) is known to mediate non-neuronal 5-HT biosynthesis, including in IECs (Walther et al., 2003). By using *Vil1*^{cre}*Tph1*$^{fl/fl}$ mice, we verified that loss of Tph1 in IECs completely abolished IL-33-induced peripheral 5-HT release (Figure 4C). Blockade of 5-HT receptors or loss of IEC-derived Tph1 repressed IL-33-induced enteric neuronal activation (Figure 4D and 4E). *Vil1*^{cre}*Tph1*$^{fl/fl}$ mice exhibited compromised colonic transit time compared to *Tph1*$^{fl/fl}$ control mice (Figure S4B and S4C). We also confirmed that IL-33-induced gut motility was 5-HT dependent (Figure 4F and 4G). Additionally, elevated serum 5-HT were seen in response to IL-33 injection in both *Il4*$^{-/-}$*Il13*$^{-/-}$ and *Rag2*$^{-/-}$*Il2rg*$^{-/-}$ mice, suggesting that in addition to type 2 immune responses, IL-33 promotes *T. muris* clearance through induction of 5-HT release from EC cells which subsequently enhances gut contractility (Figure 1, S4D and S4E).

EC cell-derived ST2 responds to IL-33 for 5-HT release.

As EC cells are the main source of peripheral 5-HT (Gershon, 2013; Gershon and Tack, 2007), we investigated the role of ST2 signaling in EC cells. We found colocalization of 5-HT and ST2, together with an EC cell marker, chromogranin A (ChgA) (Bellono et al., 2017) on the intestinal tissue (Figure 5A). By using *Chga*$^{cre\text{ER-GFP}}$ mice, we were able to specifically delete ST2 in EC cells (Figure S5A). We showed that loss of ST2 did not impact EC cell generation (Figure S5B and S5C), nor altered 5-HT biosynthesis genes expression (Figure S5D). ST2 deficiency in EC cells resulted in reduced serum 5-HT (Figure 5B), and compromised colonic contractibility (Figure S5E and S5F). More importantly, *Chga*$^{cre\text{ER}}$*Il1rl1*$^{fl/fl}$ mice exhibited completely abolished IL-33-induced 5-HT release, neuronal activation and gut motility compared to control *Il1rl1*$^{fl/fl}$ mice (Figure 5B–5F). Altogether, these data suggest that EC cell-derived ST2 signaling is mainly responsible for IL-33-mediated 5-HT secretion.

Given the significance of peristaltic movement in parasite clearance, we infected *Chga*$^{cre\text{ER}}$*Il1rl1*$^{fl/fl}$ mice with *T. muris*. Naïve *Chga*$^{cre\text{ER}}$*Il1rl1*$^{fl/fl}$ mice showed normal amounts of goblet cells and intestinal type 2 cytokines compared to *Il1rl1*$^{fl/fl}$ controls (Figure S5G–S5I). After *T. muris* infection, we also noticed similar amounts of intestinal type 2 cytokines and goblet cell hyperplasia between *Il1rl1*$^{fl/fl}$ and *Chga*$^{cre\text{ER}}$*Il1rl1*$^{fl/fl}$ mice, suggesting that loss of ST2 in EC cells did not impact type 2 immunity during parasite infection (Figure 5G–5I). Nevertheless, we observed compromised *T. muris* clearance in the large intestines from *Chga*$^{cre\text{ER}}$*Il1rl1*$^{fl/fl}$ mice pretreated with tamoxifen compared with *Il1rl1*$^{fl/fl}$ controls (Figure 5J). Moreover, kinetics study showed compromised *T. muris* clearance in *Chga*$^{cre\text{ER}}$*Il1rl1*$^{fl/fl}$ mice at both day 14 and 21 compared to *Il1rl1*$^{fl/fl}$ mice, suggesting IL-33-mediated 5-HT release is important for *T. muris* clearance in addition to type 2 immune responses (Figure S5J). Altogether, these data indicate that EC cell-derived ST2 signaling is critical for promoting intestinal peristalsis and host defense in a type 2 immune response-independent manner.

TRPA1 is required for IL-33-mediated 5-HT release.

We then asked how IL-33 induces 5-HT release from EC cells. 5-HT release requires Ca^{2+} influx ($[Ca^{2+}]_i$) via activation of various EC sensory receptors including TRPA1, olfactory receptor 558 (Olfr558), and TRPC4 (Bellono et al., 2017; Racke et al., 1996). Since ST2 alone was not sufficient to induce a $[Ca^{2+}]_i$ response by IL-33 (Figure 6A), we hypothesized that ST2 signaling might activate one of the sensory receptors to induce $[Ca^{2+}]_i$ response and 5-HT release. We found only co-expression of ST2 and TRPA1 triggered a robust $[Ca^{2+}]_i$ response upon IL-33 stimulation, suggesting that TRPA1 might be involved in IL-33-mediated 5-HT release (Figure 6A and S6A). To further address how the ST2-TRPA1 axis in EC cells regulates 5-HT release, we disassociated EC cells from the intestine of *Tph1*^{CFP} mice and found that IL-33 treatment induced membrane depolarization and action potential firing in EC cells by whole-cell patch-clamp recordings (Figure 6B). Addition of the TRPA1 antagonist A967079 or genetic deletion of TRPA1 on EC cell diminished IL-33-induced depolarization (Figure 6B and 6C), suggesting that TRPA1 is required for IL-33-induced EC cell activation.

Next, we generated intestinal organoids and differentiated them into EC cell-enriched organoids (Basak et al., 2017) from *Tph1*^{CFP}, *Il1rl1*$^{-/-}$ *Tph1*^{CFP} and *Trpa1*$^{-/-}$ *Tph1*^{CFP} mice, respectively (Figure S6B). After 8 hours of treatment, we found that IL-33 promoted 5-HT release in *Tph1*^{CFP} but not *Il1rl1*$^{-/-}$ *Tph1*^{CFP} organoids, while allyl isothiocyanate (AITC), a TRPA1 agonist, promoted 5-HT release from both *Tph1*^{CFP} and *Il1rl1*$^{-/-}$ *Tph1*^{CFP} organoids. More importantly, loss of TRPA1 abolished both IL-33 and AITC-induced 5-HT release (Figure 6D). We also confirmed that stimulations of IL-33 and AITC did not alter 5-HT biosynthesis (Figure S6C). Additionally, by using A967079 or the Ca^{2+} channels blockage ω-agatoxin IVA, we observed inhibition of 5-HT release (Figure 6E and S6D). These data indicate that the ST2-TRPA1 axis is critical for EC cell activation and 5-HT release.

To further illustrate ST2-TRPA1 signaling in 5-HT release *in vivo*, we examined and found colocalization of ST2 and TRPA1 in intestinal EC cells (Figure 6F). TRPA1 deficient mice showed abolished IL-33-induced 5-HT release and colon motility (Figure S6E and S6F). By generating *Chga*$^{cre\text{ER}}$ *Trpa1*$^{fl/fl}$ mice, we confirmed that the inducible deletion of TRPA1 in EC cells did not affect EC cell development and 5-HT biosynthesis (Figure S6G–S6I), but caused compromised intestinal tissue contraction (Figure S6J and S6K). More importantly, similar to *Trpa1*$^{-/-}$ mice, *Chga*$^{cre\text{ER}}$ *Trpa1*$^{fl/fl}$ mice showed diminished IL-33-induced 5-HT release and enteric neuron activation, resulting in impaired gut motility (Figure 6G–6K). These data indicate that EC cell-derived TRPA1 is essential for IL-33-mediated 5-HT release and gut motility.

IL-33 induces PLC-γ1 activation for 5-HT release in EC cells.

We next investigated the molecular mechanism of how IL-33-ST2 signaling activates TRPA1 channel to induce 5-HT release. We hypothesized that ST2 signaling induces intracellular Ca^{2+} increase as Ca^{2+} can directly activate TRPA1 as an endogenous ligand (Zurborg et al., 2007). Indeed, chelating intracellular Ca^{2+} with the calcium chelator BAPTA diminished IL-33-induced EC cell depolarization (Figure 7A and 7B). A previous study has shown that activation of phospholipase C (PLC) triggers endoplasmic reticulum (ER) Ca^{2+} release (Putney and Tomita, 2012). ST2 possesses a similar intracellular Toll and IL-1 receptor (TIR) domain to Toll-like receptor 4 (TLR4) (Lopetuso et al., 2013), which could potentially induce activation of PLC-γ (Zhou et al., 2015). Therefore, we hypothesized that ST2 signaling might induce activation of PLC-γ, leading to an intracellular Ca^{2+} increase. By transfecting NIH 3T3 cells with *Il1rl1* (encoded as ST2), we found enhanced phosphorylated PLC-γ1 (p-PLC-γ1) signal under IL-33 stimulation, while no p-PLC-γ2 signal was detected (Figure S7A and data not shown).

Consistently, we observed enhanced p-PLC-γ1 in primary EC cell-enriched intestinal organoids cocultured with IL-33 (Figure 7C), suggesting that PLC-γ1 acts as a downstream signal of ST2. By whole cell patch, we demonstrated that PLC-γ1 inhibitor U-73122 abolished IL-33-induced EC cell depolarization, indicating that PLC-γ1 signaling is critical for IL-33-induced EC cell activation (Figure 7D and 7E). IL-33-induced 5-HT release was diminished in the presence of U-73122 or BAPTA-AM (which is cell-permeant) in EC cell-enriched organoids (Figure 7F) without affect 5-HT biosynthesis (Figure S7B). These results

demonstrate that IL-33-ST2 signaling activates PLC-γ1 and increases intracellular Ca^{2+} to control 5-HT secretion from EC cells.

Since a previous study has indicated that the IL-33-ST2 axis activates downstream signaling cascades via MyD88 (Schmitz et al., 2005), we also examined the role of MyD88 in IL-33-mediated EC activation. Primary EC cell-enriched intestinal organoids from *Myd88*$^{-/-}$ mice still exhibited enhanced p-PLC-γ1 under IL-33 stimulation (Figure S7C and 7G), indicating that IL-33-induced PLC-γ1 activation was MyD88 independent. Plus, we found elevated 5-HT secretion in both WT and *Myd88*$^{-/-}$ EC cell-enriched intestinal organoids in response to IL-33 treatment (Figure 7H and S7D). Inhibition of PLC-γ1 diminished IL-33-induced 5-HT secretion from *Myd88*$^{-/-}$ intestinal organoids (Figure S7E and S7F). *In vivo* tests showed similar serum 5-HT and gut motility between *Myd88*$^{fl/fl}$ and *Chga*^{cre}^{ER}*Myd88*$^{fl/fl}$ mice under steady state. Meanwhile, they both exhibited elevated serum 5-HT and gut motility after IL-33 treatment (Figure S7G and S7H). These data indicate that intrinsic MyD88 is not involved in the IL-33-ST2 signaling cascade for 5-HT secretion in EC cells.

To extend our studies to humans, we investigated whether the IL-33-ST2 axis also promotes peripheral 5-HT release in the human intestine. We confirmed the co-expression of ST2 and TRPA1 on human colonic tissues (Figure 7I). By using human induced pluripotent stem cells (iPSCs), we generated EC cell-enriched human intestinal organoids (Figure S7I). In response to IL-33 stimulation, we observed enhanced p-PLC-γ1 (Figure 7J), and 5-HT release from human intestinal organoids with IL-33 stimulation (Figure 7K), but 5-HT biosynthesis was not affected (Figure S7J). We also observed that TPRA1 and Ca_V channel blockers both inhibited IL-33-induced 5-HT secretion (Figure 7K and S7J). Moreover, consistent with mouse intestinal organoid data, we found that inhibition of PLC-γ1 or chelation of intracellular Ca^{2+} diminished IL-33-induced 5-HT release, suggesting that the IL-33-ST2-TRPA1 axis also depends on PLC-γ1 signaling to regulate 5-HT secretion in human EC cells (Figure 7L, S7J and S7K).

Discussion

Gut-derived 5-HT is known to coordinate the dynamic balance between the intestinal enteroendocrine system, immune system and nervous system for intestinal and systemic homeostasis. By detecting various environmental stimuli (Bellono et al., 2017), EC cells function as one major source of peripheral 5-HT (Yano et al., 2015), but how immune signals are sensed by EC cells for 5-HT release is incompletely illustrated. As one critical alarmin cytokine, IL-33 has been recognized to regulate mucosal homeostasis and allergic responses on barrier sites including the intestinal epithelium (Kearley et al., 2015; Oliphant et al., 2011). We demonstrate here that IL-33-ST2 signaling selective promoted EC cell-derived 5-HT secretion. IL-33 triggered calcium influx for 5-HT release via a PLC-γ1-TRPA1 signaling pathway. Blockade of PLC-γ1 or TRPA1 repressed IL-33-induced 5-HT secretion in both mouse and human EC cells.

The intestinal epithelium is the interface between external environments and gut tissues, experiencing fast turnover due to the constant external challenges (Creamer et al., 1961). IL-33 is constitutively expressed and released from damaged tissues or necrotic barrier cells,

including intestinal IECs. During intestinal inflammation, elevated IL-33 expression and production can be seen on the intestinal epithelial barrier (Pichery et al., 2012; Sedhom et al., 2013). Meanwhile, IL-33 expression associates with increased type 2 immunity during infection and allergic responses (Lohning et al., 1998; Lott et al., 2015; Molofsky et al., 2015), which could lead to EC cell hyperplasia (Motomura et al., 2008; Wang et al., 2007). Our findings complement the previous studies and demonstrate that IL-33 exerts unique dual roles for both long-term EC cell development and an instantaneous EC cell response of 5-HT release. Also, given that increased gut motility has been found to facilitate the clearance of the toxins and dead cell bodies (Bercik et al., 2002; Vallance et al., 1998), our findings here demonstrate that in addition to immune regulation, IL-33 promotes the gut expulsion to restrain the inflammatory activities.

It is known that IL-33 signaling leads to IL-1R-associated kinase 4 (IRAK4) activation via MyD88 (Schmitz et al., 2005). Loss of MyD88 abolishes IL-33-promoted type 2 immunity (Ho et al., 2007; Kroeger et al., 2009; Kurowska-Stolarska et al., 2008). Prolonged treatment with IL-33 alters intestinal smooth muscle contraction due to type 2 immune responses which is also MyD88-dependent (Yang et al., 2013), while such effects are rather long term. Additionally, although MyD88 deficiency leads to compromised EC cell generation and 5-HT production *in vivo* (Wang et al., 2019), by using $Chga^{creER}Myd88^{fl/fl}$ mice, our findings suggest that intrinsic MyD88 does not directly interfere with IL-33-mediated EC cell function of 5-HT release and acute gut motility. Therefore, IL-33 could regulate gut motility through both MyD88-dependent and independent manners.

IL-33-ST2 signaling has been described to be important for DRG neuron activation, regulating sensory processes of pain and itch (Han et al., 2013; Liu et al., 2016; Zarpelon et al., 2016). General blockade of TRP channel by ruthenium red inhibits IL-33-mediated neuronal responses within DRG neurons, which is consistent with our discovery of the role of TRPA1 in IL-33-promoted 5-HT release in EC cells (Liu et al., 2016). This suggests that EC cells might share similar IL-33-induced neuronal responses and signaling pathways with neurons. Hence, regardless non-neuronal and neuronal 5-HT are generated via distinct mechanisms (Walther et al., 2003), it is possible that serotonergic neurons can also respond to IL-33 for 5-HT release regardless of their distinct 5-HT biosynthesis mechanisms from the periphery.

Dysregulation of 5-HT leads to various pathological consequences. For instance, chemotherapy-induced GI dysmotility, nausea and vomiting are known to be mediated via vagal afferent and enteric nerves activated by peripheral 5-HT (Gershon and Tack, 2007; Gregory and Ettinger, 1998). Chemotherapeutic agents are also known to cause enhanced IEC apoptosis and increase IL-33 release in the gut (Guabiraba et al., 2014). These findings line up with our discoveries of IL-33-ST2 signal promoting 5-HT release for intestinal peristaltic movement. On the other hand, 5-HT has been shown to play an important role for neurodevelopment at early stages (Bonnin et al., 2011), while IL-33 has been discovered to participate in neural circuit development (Vainchtein et al., 2018). Considering our finding of IL-33-induced 5-HT release, it is possible that IL-33 also mediates synapse homeostasis via modulation of the brain serotonergic system during development.

In this study, we have shown that the IL-33-ST2 axis plays a critical role in EC cells for 5-HT release to regulate intestinal homeostasis and host defense. Importantly, we demonstrated that in both mouse and human EC cells, IL-33 signaling selectively activated TRPA1 channels in EC cell via PLC-γ1 to promote Ca^{2+} influx and 5-HT release, indicating a causative effect of immune regulation on instantaneous neuroendocrine responses rather than consequence of altered transcription programs or development. We here address the significance of IL-33 in conducting a non-canonical immuno-neuroendocrine signaling pathway to control the rapid release of 5-HT and maintain GI physiology independent from type 2 immunity. These results thereby provide potential therapeutic strategies to the disorders associated with peripheral 5-HT dysregulation.

STAR Methods

Lead Contact—Further information and requests for resources and reagents should be directed to and will be fulfilled by the Lead Contact, Chuan Wu (chuan.wu@nih.gov).

Materials Availability—This study did not generate new unique reagents.

Data and Code Availability—This study did not generate any unique datasets or code.

EXPERIMENTAL MODEL AND SUBJECT DETAILS

Mice—C57BL/6J (WT), *Cd4*^{Cre}, *Plzf*^{Cre}, *Cx3Cr1*^{CreER}, *Cpa3*^{Cre}, *Phox2b*^{Cre}, *Gfap*^{Cre}, *Acta2*^{Cre}, *Lgr5*^{CreER}, *Vil1*^{Cre}, *Trpa1*$^{-/-}$, Myd88$^{-/-}$, and *Myd88*^{flox} mice were purchased from Jackson Laboratory; *Il33*$^{-/-}$ mice were from Dr. Susumu Nakae; Dr. *Pirt*^{GCaMP3} and *Pirt*^{Cre} mice were from Dr. Xinzhong Dong; *Ret*^{CreER} mice were from Dr. David; *Trpa1*^{flox} mice were from Dr. Cheryl L. Stucky; *Hand2*^{Cre} mice were from Dr. David E. Clouthier; *Tph1*^{flox} mice were from Dr. Gerard Karsenty; *Tph1*^{CFP} mice were from Dr. Andrew B. Leiter; *Mcpt5*^{Cre} mice were from Dr. Axel Roers; *Il4*$^{-/-}$*Il13*$^{-/-}$ mice were from NIAID-Taconic repository; *Il1rl1*^{flox} mice were from KOMP; *Chga*$^{CreER\text{-}GFP}$ mice were from EMMA. The heterozygous Il33+/− mice were used for Il33 GFP reporter mice. Details about the generation of the Il1rl1−/−mice have not been published. The information about this line is available from G.T. upon request.

Mouse lines were interbred in our facilities to obtain the final strains described in the text. Mice were maintained at the National Cancer Institute facilities under specific pathogen-free conditions. Mice were fed a standard chow diet and used at 7–12 weeks of age for most experiments. All experiments were carried out in accordance with guidelines prescribed by the Institutional Animal Care and Use Committee at the National Cancer Institute. For *Chga*^{CreER}*Il1rl1*$^{fl/fl}$, *Chga*^{CreER}*Trpa1*$^{fl/fl}$, or *Chga*^{CreER}*Myd88*$^{fl/fl}$ *mice,* 1mg Tamoxifen was i.p. injected daily for 5 days before the experiments.

METHOD DETAILS

T. muris* infection—Trichuris muris* were maintained in susceptible *Stat6*$^{-/-}$ mice. Mice were inoculated with approximately 300 infective eggs by oral gavage. After 7, 14, or 21 days as indicated, the mice were sacrificed, and the cecum and colon tissues were isolated

and opened longitudinally with scissors. The fecal material was rinsed from the tissues with warm PBS and the tissue incubated at 37C in PBS for 3 hours followed by a brief vortex of the tissues to remove the epithelial layer. Larval worm burdens were counted in the suspension by dissecting microscope. For IL-33 administration, 200 ng mouse recombinant IL-33 (Biolegend) was i.p. injected daily from day 9 to day 13 post infection.

Bead expulsion assay—For colonic propulsion measurement, mice were deprived of the food with access to water overnight for 12 hrs on the first day. Before the experiment, the mouse was performed with anesthesia (2.5% Isoflurane), a 2 mm diameter glass bead was inserted into the rectum in the depth of 2 cm from the anus with an oil-polished glass rod. After the mouse was put back into the cage, the mouse was monitored, and the time of the bead expulsion was recorded. The distal colonic transit time was determined by monitoring the time required for the expulsion of the glass bead. Control and experimental groups were age and sex matched. For IL-33 administration, 200 ng mouse recombinant IL-33 (Biolegend) was administered by i.p. injections prior to the assay.

Mouse antibiotic treatment—Adult WT, *Il33*$^{-/-}$ and *Il1rl1*$^{-/-}$ mice were given antibiotics cocktail (1 g/L Ampicillin, 1 g/L Neomycin, 1 g/L Metronidazole, 0.5 g/L Vancomycin) in drinking water for 4 weeks. After the mouse stool samples are confirmed as sterile in agar plate incubation, the mice were tested for colonic bead expulsion assay.

ELISA—For cytokine measurement, mesenteric lymph nodes (MLN) were harvested and meshed for single cell suspension. The cells were cultured in RPMI media in the plates coated with 1 μg/ml anti-CD3 and anti-CD28 (BioXcell) for 3 days. The IL-4, IL-5 and IL-13 cytokines were quantified from the culture media using DuoSet ELISA (R&D) according to the manufacturer's protocol.

For serotonin and other secretomics analysis, the blood samples were collected by cardiac puncture and the serum was isolated. The measurements were performed using Serotonin ELISA Kit (Abnova), Motilin (MTL) ELISA Kit (American Research Products, Inc.), Mouse CCK EIA, Mouse GLP-1 EIA, Mouse PYY EIA, Mouse Neurotensin EIA and Mouse GIP EIA (RayBiotech), according to the manufacturers' protocols.

CMMC (colonic migrating motor complex) recording—CMMC recording was performed according to previously described (Spencer, 2013). Briefly, the entire mouse colon was removed and transferred to a dish containing warm (35 ± 1°C) Krebs solution: 120 mM NaCl, 5.9 mM KCl, 14.4 mM $NaHCO_3$, 1.2 mM $MgCl_2$, 1.35 mM NaH_2PO_4, 11.5 mM glucose, 2.5 mM $CaCl_2$ (pH 7.4) bubbled with 95%O_2/5%CO_2. The contraction of circular muscle during each CMMC was recorded using independent isometric force transducers (AD instruments) connected via fine suture thread to hooks that pierced the muscle wall at the proximal, middle and distal region of the colon. Each transducer was connected to an input channel of the bridge amplifier (AD instruments). Data were acquired using the PowerLab data acquisition system operated by LabChart software (AD instruments).

Calcium imaging—The mouse colon was removed and cut open along the mesenteric border. The tissue was pinned flat with mucosal side uppermost to the bottom of a 35 mm dish coated with Sylgard-184 (Dow Corning Corp., Midland, MI, USA). Tissue was bathed in Krebs solution containing 120 mM NaCl, 5.9 mM KCl, 14.4 mM $NaHCO_3$, 1.2 mM $MgCl_2$, 1.35 mM NaH_2PO_4, 11.5 mM glucose, 2.5 mM $CaCl_2$ (pH 7.4). The epithelium layer was removed under a dissecting microscope when indicated. The time-lapse movies of whole mount calcium imaging data were acquired with NIS-elements software using an inverted confocal microscope (Nikon). Data were processed and analyzed using ImageJ software (NIH) (Schneider et al., 2012).

Cultured NIH 3T3 cell transfected with ST2, TRPA1, TRPC4 or Olfr558 were loaded with 4 μM Fura-2 AM (Invitrogen) in culture medium at 37 °C for 45 min. Cells were then washed three times with calcium imaging buffer (135 mM NaCl, 5 mM KCl, 2 mM $CaCl_2$, 0.5 mM $MgCl_2$, 0.5 mM $MgSO_4$, 0.44 mM KH_2PO_4, 0.34 mM Na_2HPO_4, 10 mM HEPES, 10 mM glucose, 30 mM sucrose, pH 7.45) and analyzed 30 min later. Calcium-free imaging buffer was prepared by replacing $CaCl_2$ with 1 mM EGTA (Sigma-Aldrich). Murine IL-33 (Biolegend) were used at 300 nM, while Ionomycin (Sigma), AITC (Sigma-Aldrich), Isovalerate (Sigma) were used at 10 μM, 100 μM, and 100 μM, respectively, unless otherwise indicated. Fluorescence at 340 nm and 380 nm excitation wavelengths (F340, F380) was recorded using an inverted Nikon Ti-S microscope with NIS-Elements imaging software (Nikon Instruments). The ratio of fluorescence intensities (F340/F380) was used to reflect changes in $[Ca^{2+}]_i$ values on stimulation. The threshold of activation was defined as three standard deviations above the average.

Intestinal histology and immunofluorescence staining—Mouse colon was fixed in 10% neutral formalin and stored in 70% ethanol. Intestinal samples were then paraffin-embedded and cut into 10 um longitudinal sections, and the PAS staining was performed by Histoserv Inc. (Germantown, MD). Goblet cells were counted and calculated from 10 crypts in each slide.

For immunofluorescence staining, slides were deparaffinized by xylene and antigen retrieval was conducted for 20 min in a 95°-water bath in 10 mM sodium citrate, pH 6.0 followed by a 15 min incubation at room temperature. Slides were washed, blocked in 5% bovine serum albumin, and stained with the primary antibodies, anti-ChgA (1:100; Abcam), anti-5-HT (1:100; Abcam), anti-ST2 (1:100, Proteintech) and anti-TRPA1 (1:100, Novus) and secondary antibodies conjugated to Alexa fluor 488, 633 or 594 (Thermo Fisher). Slides were mounted in Fluoromount-G (Thermo Fisher), and 3–15 images were taken per slide at 20X or 40X magnification along transections of the intestinal crypts for each biological replicate (Zeiss). For 5-HT and ChgA staining, numbers of positively stained puncta were scored blindly, normalized to total area of intestinal mucosa using ImageJ software (NIH), and then averaged across biological replicates.

iDISCO (Whole-mount intestine immunofluorescence)—The iDISCO protocol was performed according to the protocol on the continuously updated website htpp://idisco.info. Briefly, the colon tissues were cut longitudinally and fixed with 4% PFA. After washing and methanol dehydration steps, whole mount samples were permeabilized first in 0.2% Triton

X-100 followed by 0.2% Triton X-100/20% DMSO/0.3M Glycine. The samples were blocked for 1–2 days in 1X DPBS with 0.2% Triton X-100 / 10% DMSO / 6% Donkey Serum at 37° with gentle agitation. anti-GFP (1:500, Abcam), anti-β-Tubulin III (1:100, Biolegend) antibodies and fluorescence conjugated secondary antibodies were added to the blocking buffer at appropriate concentrations and incubated 1–2 days at 37. Samples were then washed in 1X DPBS with 0.2%Tween-20 and Heparin (100 mg/ml), mounted in agarose and cleared using dichloromethane followed by benzyl ether. Images were taken by Confocal microscope (Zeiss) and analyzed by Imaris.

Flow cytometry—Colon tissues were isolated and were opened longitudinally. The intestinal epithelial cells were harvested after the tissues were incubated at 37 °C for 20 min in PBS media containing 10%FBS, 5 mM EDTA and 1 mM DTT. The isolated epithelial cells were stained with APC-anti-EpCam (1:100, Biolegend), BV421-anti-ST2 (1:100, Biolegend) and viability dye PI (BD). All flow cytometry data were acquired on a BD LSRFortessa™ X-20 cell analyzer and analyzed with FlowJo software.

Primary culture of EC cell—EC cells were cultured according to previously described (Knutson et al., 2018). In brief, *Tph1*^{CFP} transgenic mice were euthanized and the colon was removed. After flushing out the luminal contents, the full thickness tissue was inverted and chopped into small pieces. Wash the pieces three times with ice-cold PBS. The tissue was digested with Collagenase type XI (0.6 mg/mL) at 37 °C in DMEM containing 0.1% BSA in 4 separate digestions for a total of 40 min. Supernatants from the last two digestions were collected and centrifuged at 100 g for 5 min. Cell pellet was resuspended at 1×10^6/ml in DMEM containing 5% Heat Inactivated FBS, 1% Pen-step, 1% L-Glutamine, and 10 μM Y-27632. Cells were plated on coverslips coated with 5% w/v Matrigel. Cells were maintained in standard culture conditions for 24–48 hours.

Patch-clamp recording—Whole-cell patch-clamp recordings were performed at room temperature (22–24 °C) on the stage of an inverted microscope equipped with fluorescence filter set for the visualization of CFP. Pipettes pulled from borosilicate glass (BF 150-110-10) with a Sutter P-1000 puller (Sutter) had resistances of 2–5 MΩ when filled with intracellular solution containing 140 mM KCl, 1 mM $MgCl_2$, 5 mM EGTA, 3 mM ATP, 10 mM HEPES (pH 7.2 adjusted with KOH). The extracellular solution contained 140 mM NaCl, 5 mM KCl, 1 mM $MgCl_2$, 2.5 mM $CaCl_2$, 10 mM HEPES, 10 mM Glucose (pH 7.4 adjusted with NaOH). After establishing the whole-cell recording configuration, membrane potential data were acquired in current-clamp mode using Clampex 10 software (Molecular Devices) and analyzed with pClamp 10.6 (Molecular Devices). Data were sampled at 10 kHz and filtered at 2 kHz.

Intestinal organoids generation—*Tph1*^{CFP} mice aged 6–10 weeks were used to generate intestinal organoids, as previously reported (Sato et al., 2009). Briefly, the small intestine was isolated and washed with cold PBS and crypts were isolated following dissociation in EDTA. Isolated crypts were suspended in Matrigel. Following polymerization, IntestiCult™ Organoid Growth Medium (Stemcell) was added and refreshed every 3–4 days. Organoids were maintained at 37 °C, 5% CO2 and propagated weekly. For

the induction of EC cell enriched differentiation, organoids were cultured in standard culture conditions plating in Matrigel for 2 days. The organoids were cultured in the media the cocktails for EC cell enriched differentiation including IWP2 (1.5 mM; Sigma Aldrich), DAPT (10 mM, Sigma Aldrich) and MEK inhibitor PD0325901 (1 mM; Sigma Aldrich) for 7 days. For serotonin measurement, the media was harvested before the treatments and used as control in the quantification of the 5-HT amounts after the treatments.

Western blot—The transfected NIH 3T3 cells were lysed in whole cell extract buffer (50 mM Tris-HCl, pH 7.5, 150 mM NaCl, 1% NP-40, 0.2 mM EDTA, 10 mM Na_3VO_4, 10% glycerol, protease inhibitors). Proteins were separated by gel electrophoresis using 4–12% NuPAGE Bis-Tris gels (Genscript) followed by transfer to nitrocellulose membrane. Membranes were incubated with 5% milk in TBST (0.5 M NaCl, Tris-HCl, pH 7.5, 0.1% (v/v) Tween-20) for 60 min and washed once with TBST. Proteins of interest were detected by incubating membranes over night at 4°C in blocking buffer with anti-p-PLCγ1 (Cell Signaling), anti-PLCγ1 (Cell Signaling), or anti-β-Actin (Sigma), washing with TBST three times for 10 min and incubating with horseradish peroxidase-conjugated anti-rabbit or anti-mouse antibody (Cell Signaling). Blotting signaling was detected with SuperSignal™ West Pico PLUS Chemiluminescent Substrate (Thermo Fisher).

Quantitative RT-PCR—For gene expression detection, total RNA was isolated from whole cells using the Qiagen miniRNA extraction kit following the manufacturer's instructions. RNA was quantified and complementary DNA was reverse-transcribed using the iScript kit (Biorad) following the manufacturer's instructions. The cDNA samples were used at 20ng/well in a 384 well plate and run in triplicate. PCR reactions were set up using TaqMan Universal PCR Master Mix (Applied Biosystems) on an ABI Prism 7500 Sequence Detection System. Quantification of relative mRNA expression was normalized to the expression of β-Actin.

Human iPSC derived intestinal organoids—The human iPSC line ND1.4 derived from human fibroblast was got from iPSC core in National Heart, Lung, and Blood Institute (NHLBI). The iPSCs were maintained in the feeder free Essential 8™ Medium (Thermo Fisher) on Matrigel. The differentiation from iPSCs into intestinal organoids were performed with STEMdiff™ Intestinal Organoid Kit (Stemcell) according to the manufacturer's instructions. The human intestinal organoids were cultured in STEMdiff™ Intestinal Organoid Growth Medium (Stemcell) in Matrigel. The organoids were differentiated into EEC with the addition of IWP2 (1.5 mM; Sigma Aldrich), DAPT (10 mM, Sigma Aldrich) and MEK inhibitor PD0325901 (1 mM; Sigma Aldrich) in media. All human subjects studies were performed under signed consent and approved by the NIH Review Board (IRB), PRD #7169.

Quantification and Statistical Analysis—Statistical analyses were performed with Graphpad Prism 5.0 (Graph Pad software, La Jolla, CA, USA) using an unpaired two-tailed Student's t-test. Statistical significance was defined as $P < 0.05$.

Supplementary Material

Refer to Web version on PubMed Central for supplementary material.

Acknowledgements

We thank Dr. Susumu Nakae (The University of Tokyo, Japan) for *Il33*$^{-/-}$ mice; Dr. Xinzhong Dong (Johns Hopkins School of Medicine) for the *Pirt*$^{\text{GCaMP3}}$ and *Pirt*^{cre} mice; Dr. David Ginty (Harvard Medical School) for the *Ret*$^{cre\text{ER}}$ mice; Dr. Cheryl L. Stucky (Medical College of Wisconsin) for the *Trpa1*$^{\text{flox}}$ mice; Dr. David E. Clouthier (University of Colorado Denver) for the *Hand2*^{cre} mice; Dr. Gerard Karsenty (Columbia University) for the *Tph1*$^{\text{flox}}$ mice; Dr. Andrew B. Leiter (University of Massachusetts Medical School) for the *Tph1*$^{\text{CFP}}$ mice; Dr. Axel Roers (Dresden University of Technology, Germany) for the *Mcpt5*^{cre} mice;. We thank Mr. Eric Chen and Dr. Jagan Muppidi (NIH/NCI) for editing the manuscript. National Multiple Sclerosis Society Career Transition Award (TA 3059-A-2 to C.W.).

References:

Alcaino C, Knutson KR, Treichel AJ, Yildiz G, Strege PR, Linden DR, Li JH, Leiter AB, Szurszewski JH, Farrugia G, and Beyder A (2018). A population of gut epithelial enterochromaffin cells is mechanosensitive and requires Piezo2 to convert force into serotonin release. Proceedings of the National Academy of Sciences of the United States of America 115, E7632–E7641. [PubMed: 30037999]

Antignano F, Mullaly SC, Burrows K, and Zaph C (2011). Trichuris muris infection: a model of type 2 immunity and inflammation in the gut. J Vis Exp.

Baganz NL, and Blakely RD (2013). A dialogue between the immune system and brain, spoken in the language of serotonin. ACS Chem Neurosci 4, 48–63. [PubMed: 23336044]

Basak O, Beumer J, Wiebrands K, Seno H, van Oudenaarden A, and Clevers H (2017). Induced Quiescence of Lgr5+ Stem Cells in Intestinal Organoids Enables Differentiation of Hormone-Producing Enteroendocrine Cells. Cell Stem Cell 20, 177–190 e174. [PubMed: 27939219]

Bellono NW, Bayrer JR, Leitch DB, Castro J, Zhang C, O'Donnell TA, Brierley SM, Ingraham HA, and Julius D (2017). Enterochromaffin Cells Are Gut Chemosensors that Couple to Sensory Neural Pathways. Cell 170, 185–198 e116. [PubMed: 28648659]

Bercik P, De Giorgio R, Blennerhassett P, Verdu EF, Barbara G, and Collins SM (2002). Immune-mediated neural dysfunction in a murine model of chronic Helicobacter pylori infection. Gastroenterology 123, 1205–1215. [PubMed: 12360482]

Bonnin A, Goeden N, Chen K, Wilson ML, King J, Shih JC, Blakely RD, Deneris ES, and Levitt P (2011). A transient placental source of serotonin for the fetal forebrain. Nature 472, 347–350. [PubMed: 21512572]

Burzyn D, Kuswanto W, Kolodin D, Shadrach JL, Cerletti M, Jang Y, Sefik E, Tan TG, Wagers AJ, Benoist C, and Mathis D (2013). A special population of regulatory T cells potentiates muscle repair. Cell 155, 1282–1295. [PubMed: 24315098]

Crane JD, Palanivel R, Mottillo EP, Bujak AL, Wang H, Ford RJ, Collins A, Blumer RM, Fullerton MD, Yabut JM, et al. (2015). Inhibiting peripheral serotonin synthesis reduces obesity and metabolic dysfunction by promoting brown adipose tissue thermogenesis. Nature medicine 21, 166–172.

Creamer B, Shorter RG, and Bamforth J (1961). The turnover and shedding of epithelial cells. I. The turnover in the gastro-intestinal tract. Gut 2, 110–118. [PubMed: 13696345]

Fallon PG, Jolin HE, Smith P, Emson CL, Townsend MJ, Fallon R, Smith P, and McKenzie AN (2002). IL-4 induces characteristic Th2 responses even in the combined absence of IL-5, IL-9, and IL-13. Immunity 17, 7–17. [PubMed: 12150887]

Furness JB (2012). The enteric nervous system and neurogastroenterology. Nat Rev Gastroenterol Hepatol 9, 286–294. [PubMed: 22392290]

Furness JB, Rivera LR, Cho HJ, Bravo DM, and Callaghan B (2013). The gut as a sensory organ. Nat Rev Gastroenterol Hepatol 10, 729–740. [PubMed: 24061204]

Gabanyi I, Muller PA, Feighery L, Oliveira TY, Costa-Pinto FA, and Mucida D (2016). Neuro-immune Interactions Drive Tissue Programming in Intestinal Macrophages. Cell 164, 378–391. [PubMed: 26777404]

Gadani SP, Walsh JT, Smirnov I, Zheng J, and Kipnis J (2015). The glia-derived alarmin IL-33 orchestrates the immune response and promotes recovery following CNS injury. Neuron 85, 703–709. [PubMed: 25661185]

Gershon MD (2013). 5-Hydroxytryptamine (serotonin) in the gastrointestinal tract. Curr Opin Endocrinol Diabetes Obes 20, 14–21. [PubMed: 23222853]

Gershon MD, and Tack J (2007). The serotonin signaling system: from basic understanding to drug development for functional GI disorders. Gastroenterology 132, 397–414. [PubMed: 17241888]

Gregory RE, and Ettinger DS (1998). 5-HT3 receptor antagonists for the prevention of chemotherapy-induced nausea and vomiting. A comparison of their pharmacology and clinical efficacy. Drugs 55, 173–189. [PubMed: 9506240]

Guabiraba R, Besnard AG, Menezes GB, Secher T, Jabir MS, Amaral SS, Braun H, Lima-Junior RC, Ribeiro RA, Cunha FQ, et al. (2014). IL-33 targeting attenuates intestinal mucositis and enhances effective tumor chemotherapy in mice. Mucosal immunology 7, 1079–1093. [PubMed: 24424522]

Han P, Zhao J, Liu SB, Yang CJ, Wang YQ, Wu GC, Xu DM, and Mi WL (2013). Interleukin-33 mediates formalin-induced inflammatory pain in mice. Neuroscience 241, 59–66. [PubMed: 23523996]

Ho LH, Ohno T, Oboki K, Kajiwara N, Suto H, Iikura M, Okayama Y, Akira S, Saito H, Galli SJ, and Nakae S (2007). IL-33 induces IL-13 production by mouse mast cells independently of IgE-FcepsilonRI signals. Journal of leukocyte biology 82, 1481–1490. [PubMed: 17881510]

Humphreys NE, Xu D, Hepworth MR, Liew FY, and Grencis RK (2008). IL-33, a potent inducer of adaptive immunity to intestinal nematodes. Journal of immunology 180, 2443–2449.

Hung LY, Lewkowich IP, Dawson LA, Downey J, Yang Y, Smith DE, and Herbert DR (2013). IL-33 drives biphasic IL-13 production for noncanonical Type 2 immunity against hookworms. Proceedings of the National Academy of Sciences of the United States of America 110, 282–287. [PubMed: 23248269]

Kearley J, Silver JS, Sanden C, Liu Z, Berlin AA, White N, Mori M, Pham TH, Ward CK, Criner GJ, et al. (2015). Cigarette smoke silences innate lymphoid cell function and facilitates an exacerbated type I interleukin-33-dependent response to infection. Immunity 42, 566–579. [PubMed: 25786179]

Knutson K, Strege PR, Li J, Leiter AB, Farrugia G, and Beyder A (2018). Whole Cell Electrophysiology of Primary Cultured Murine Enterochromaffin Cells. Jove-J Vis Exp.

Kroeger KM, Sullivan BM, and Locksley RM (2009). IL-18 and IL-33 elicit Th2 cytokines from basophils via a MyD88- and p38alpha-dependent pathway. Journal of leukocyte biology 86, 769–778. [PubMed: 19451398]

Kurowska-Stolarska M, Kewin P, Murphy G, Russo RC, Stolarski B, Garcia CC, Komai-Koma M, Pitman N, Li Y, Niedbala W, et al. (2008). IL-33 induces antigen-specific IL-5+ T cells and promotes allergic-induced airway inflammation independent of IL-4. Journal of immunology 181, 4780–4790.

Launay JM, Herve P, Peoc'h K, Tournois C, Callebert J, Nebigil CG, Etienne N, Drouet L, Humbert M, Simonneau G, and Maroteaux L (2002). Function of the serotonin 5-hydroxytryptamine 2B receptor in pulmonary hypertension. Nature medicine 8, 1129–1135.

Liew FY, Girard JP, and Turnquist HR (2016). Interleukin-33 in health and disease. Nature reviews. Immunology 16, 676–689.

Liu B, Tai Y, Achanta S, Kaelberer MM, Caceres AI, Shao X, Fang J, and Jordt SE (2016). IL-33/ST2 signaling excites sensory neurons and mediates itch response in a mouse model of poison ivy contact allergy. Proceedings of the National Academy of Sciences of the United States of America 113, E7572–E7579. [PubMed: 27821781]

Lohning M, Stroehmann A, Coyle AJ, Grogan JL, Lin S, Gutierrez-Ramos JC, Levinson D, Radbruch A, and Kamradt T (1998). T1/ST2 is preferentially expressed on murine Th2 cells, independent of interleukin 4, interleukin 5, and interleukin 10, and important for Th2 effector function.

Proceedings of the National Academy of Sciences of the United States of America 95, 6930–6935. [PubMed: 9618516]

Lopetuso LR, Chowdhry S, and Pizarro TT (2013). Opposing Functions of Classic and Novel IL-1 Family Members in Gut Health and Disease. Frontiers in immunology 4, 181. [PubMed: 23847622]

Lott JM, Sumpter TL, and Turnquist HR (2015). New dog and new tricks: evolving roles for IL-33 in type 2 immunity. Journal of leukocyte biology 97, 1037–1048. [PubMed: 25801770]

Mahapatro M, Foersch S, Hefele M, He GW, Giner-Ventura E, McHedlidze T, Kindermann M, Vetrano S, Danese S, Gunther C, et al. (2016). Programming of Intestinal Epithelial Differentiation by IL-33 Derived from Pericryptal Fibroblasts in Response to Systemic Infection. Cell Rep 15, 1743–1756. [PubMed: 27184849]

Mercado CP, Quintero MV, Li Y, Singh P, Byrd AK, Talabnin K, Ishihara M, Azadi P, Rusch NJ, Kuberan B, et al. (2013). A serotonin-induced N-glycan switch regulates platelet aggregation. Sci Rep 3, 2795. [PubMed: 24077408]

Molofsky AB, Savage AK, and Locksley RM (2015). Interleukin-33 in Tissue Homeostasis, Injury, and Inflammation. Immunity 42, 1005–1019. [PubMed: 26084021]

Motomura Y, Ghia JE, Wang H, Akiho H, El-Sharkawy RT, Collins M, Wan Y, McLaughlin JT, and Khan WI (2008). Enterochromaffin cell and 5-hydroxytryptamine responses to the same infectious agent differ in Th1 and Th2 dominant environments. Gut 57, 475–481. [PubMed: 18198200]

O'Malley D, Liston M, Hyland NP, Dinan TG, and Cryan JF (2011). Colonic soluble mediators from the maternal separation model of irritable bowel syndrome activate submucosal neurons via an interleukin-6-dependent mechanism. Am J Physiol Gastrointest Liver Physiol 300, G241–252. [PubMed: 21109592]

Oliphant CJ, Barlow JL, and McKenzie AN (2011). Insights into the initiation of type 2 immune responses. Immunology 134, 378–385. [PubMed: 22044021]

Pichery M, Mirey E, Mercier P, Lefrancais E, Dujardin A, Ortega N, and Girard JP (2012). Endogenous IL-33 is highly expressed in mouse epithelial barrier tissues, lymphoid organs, brain, embryos, and inflamed tissues: in situ analysis using a novel Il-33-LacZ gene trap reporter strain. Journal of immunology 188, 3488–3495.

Putney JW, and Tomita T (2012). Phospholipase C signaling and calcium influx. Adv Biol Regul 52, 152–164. [PubMed: 21933679]

Racke K, Reimann A, Schworer H, and Kilbinger H (1996). Regulation of 5-HT release from enterochromaffin cells. Behav Brain Res 73, 83–87. [PubMed: 8788482]

Rakhilin N, Barth B, Choi J, Munoz NL, Kulkarni S, Jones JS, Small DM, Cheng YT, Cao Y, LaVinka C, et al. (2016). Simultaneous optical and electrical in vivo analysis of the enteric nervous system. Nat Commun 7, 11800. [PubMed: 27270085]

Rehn M, Hubschle T, and Diener M (2004). TNF-alpha hyperpolarizes membrane potential and potentiates the response to nicotinic receptor stimulation in cultured rat myenteric neurones. Acta physiologica Scandinavica 181, 13–22. [PubMed: 15086448]

Saito H, Chi QY, Zhuang HY, Matsunami H, and Mainland JD (2009). Odor Coding by a Mammalian Receptor Repertoire. Sci Signal 2.

Sato T, Vries RG, Snippert HJ, van de Wetering M, Barker N, Stange DE, van Es JH, Abo A, Kujala P, Peters PJ, and Clevers H (2009). Single Lgr5 stem cells build crypt-villus structures in vitro without a mesenchymal niche. Nature 459, 262–265. [PubMed: 19329995]

Schmitz J, Owyang A, Oldham E, Song Y, Murphy E, McClanahan TK, Zurawski G, Moshrefi M, Qin J, Li X, et al. (2005). IL-33, an interleukin-1-like cytokine that signals via the IL-1 receptor-related protein ST2 and induces T helper type 2-associated cytokines. Immunity 23, 479–490. [PubMed: 16286016]

Schneider CA, Rasband WS, and Eliceiri KW (2012). NIH Image to ImageJ: 25 years of image analysis. Nat Methods 9, 671–675. [PubMed: 22930834]

Sedhom MA, Pichery M, Murdoch JR, Foligne B, Ortega N, Normand S, Mertz K, Sanmugalingam D, Brault L, Grandjean T, et al. (2013). Neutralisation of the interleukin-33/ST2 pathway ameliorates experimental colitis through enhancement of mucosal healing in mice. Gut 62, 1714–1723. [PubMed: 23172891]

Spencer NJ (2013). Characteristics of colonic migrating motor complexes in neuronal NOS (nNOS) knockout mice. Front Neurosci-Switz 7.

Stasi C, Bellini M, Bassotti G, Blandizzi C, and Milani S (2014). Serotonin receptors and their role in the pathophysiology and therapy of irritable bowel syndrome. Tech Coloproctol 18, 613–621. [PubMed: 24425100]

Vainchtein ID, Chin G, Cho FS, Kelley KW, Miller JG, Chien EC, Liddelow SA, Nguyen PT, Nakao-Inoue H, Dorman LC, et al. (2018). Astrocyte-derived interleukin-33 promotes microglial synapse engulfment and neural circuit development. Science 359, 1269–1273. [PubMed: 29420261]

Vallance BA, and Collins SM (1998). The effect of nematode infection upon intestinal smooth muscle function. Parasite Immunol 20, 249–253. [PubMed: 9651926]

Vallance BA, Croitoru K, and Collins SM (1998). T lymphocyte-dependent and -independent intestinal smooth muscle dysfunction in the T. spiralis-infected mouse. The American journal of physiology 275, G1157–1165. [PubMed: 9815046]

Walther DJ, Peter JU, Bashammakh S, Hortnagl H, Voits M, Fink H, and Bader M (2003). Synthesis of serotonin by a second tryptophan hydroxylase isoform. Science 299, 76. [PubMed: 12511643]

Wang H, Kwon YH, Dewan V, Vahedi F, Syed S, Fontes ME, Ashkar AA, Surette MG, and Khan WI (2019). TLR2 Plays a Pivotal Role in Mediating Mucosal Serotonin Production in the Gut. Journal of immunology 202, 3041–3052.

Wang H, Steeds J, Motomura Y, Deng Y, Verma-Gandhu M, El-Sharkawy RT, McLaughlin JT, Grencis RK, and Khan WI (2007). CD4+ T cell-mediated immunological control of enterochromaffin cell hyperplasia and 5-hydroxytryptamine production in enteric infection. Gut 56, 949–957. [PubMed: 17303597]

Xia Y, Hu HZ, Liu S, Ren J, Zafirov DH, and Wood JD (1999). IL-1beta and IL-6 excite neurons and suppress nicotinic and noradrenergic neurotransmission in guinea pig enteric nervous system. The Journal of clinical investigation 103, 1309–1316. [PubMed: 10225974]

Yadav VK, Balaji S, Suresh PS, Liu XS, Lu X, Li Z, Guo XE, Mann JJ, Balapure AK, Gershon MD, et al. (2010). Pharmacological inhibition of gut-derived serotonin synthesis is a potential bone anabolic treatment for osteoporosis. Nature medicine 16, 308–312.

Yang Z, Sun R, Grinchuk V, Fernandez-Blanco JA, Notari L, Bohl JA, McLean LP, Ramalingam TR, Wynn TA, Urban JF Jr., et al. (2013). IL-33-induced alterations in murine intestinal function and cytokine responses are MyD88, STAT6, and IL-13 dependent. Am J Physiol Gastrointest Liver Physiol 304, G381–389. [PubMed: 23257921]

Yano JM, Yu K, Donaldson GP, Shastri GG, Ann P, Ma L, Nagler CR, Ismagilov RF, Mazmanian SK, and Hsiao EY (2015). Indigenous bacteria from the gut microbiota regulate host serotonin biosynthesis. Cell 161, 264–276. [PubMed: 25860609]

Zarpelon AC, Rodrigues FC, Lopes AH, Souza GR, Carvalho TT, Pinto LG, Xu D, Ferreira SH, Alves-Filho JC, McInnes IB, et al. (2016). Spinal cord oligodendrocyte-derived alarmin IL-33 mediates neuropathic pain. FASEB journal : official publication of the Federation of American Societies for Experimental Biology 30, 54–65. [PubMed: 26310268]

Zhang L, Hu L, Chen M, and Yu B (2013). Exogenous interleukin-6 facilitated the contraction of the colon in a depression rat model. Dig Dis Sci 58, 2187–2196. [PubMed: 23589140]

Zhou X, Ye Y, Sun Y, Li X, Wang W, Privratsky B, Tan S, Zhou Z, Huang C, Wei YQ, et al. (2015). Transient Receptor Potential Channel 1 Deficiency Impairs Host Defense and Proinflammatory Responses to Bacterial Infection by Regulating Protein Kinase Calpha Signaling. Molecular and cellular biology 35, 2729–2739. [PubMed: 26031335]

Zurborg S, Yurgionas B, Jira JA, Caspani O, and Heppenstall PA (2007). Direct activation of the ion channel TRPA1 by Ca2+. Nat Neurosci 10, 277–279. [PubMed: 17259981]

Highlights

1. IL-33-ST2 signaling regulates gut motility and intestinal host defense
2. Enterochromaffin (EC) cell-derived ST2 responds to IL-33 for 5-HT release.
3. TRPA1 is required for IL-33-mediated 5-HT release.
4. IL-33 induces PLC-γ1 activation for 5-HT release in both mouse and human EC cells.

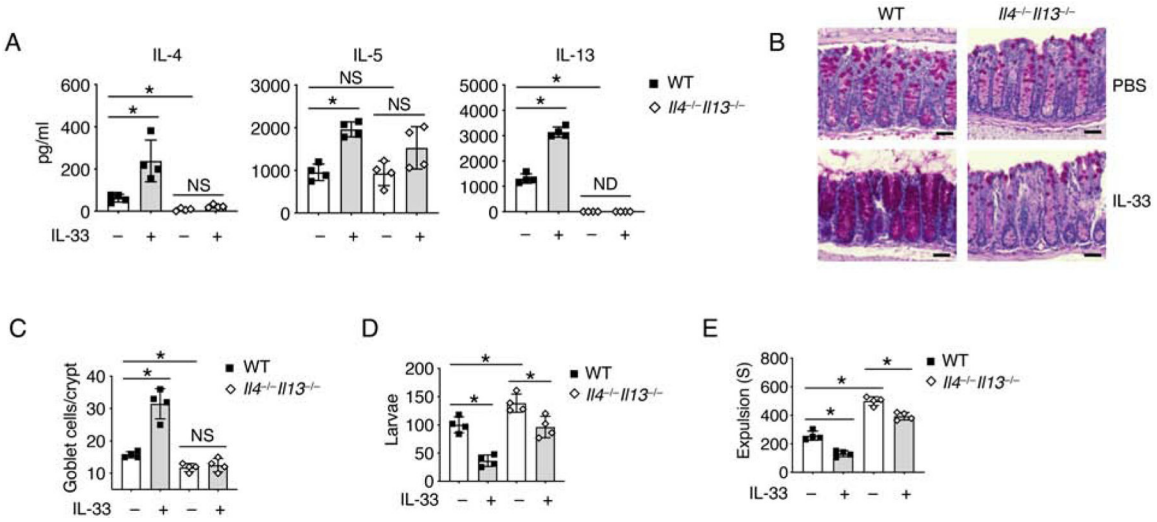

Figure 1. IL-33 promotes parasite expulsion in a type 2 immune response-independent manner.

(A-E) *T. muris* eggs were inoculated into WT and *Il4*$^{-/-}$*Il13*$^{-/-}$ mice by oral gavage. The mice were treated with PBS or IL-33 daily from day 7 and sacrificed on 14 day for further test.

(A) IL-4, IL-5 and IL-13 protein concentrations in mesenteric lymph nodes (mLN) were assessed by ELISA.

(B) PAS staining and (C) Quantification of goblet cells per crypt of colonic tissues. Scale bar, 50 μm.

(D) Quantification of larvae in the colons of WT and *Il4*$^{-/-}$*Il13*$^{-/-}$ mice.

(E) *T. muris* infected WT and *Il4*$^{-/-}$*Il13*$^{-/-}$ mice were treated daily with PBS or IL-33 for 7 days. Colonic transit time was assessed by bead expulsion assay.

Data are representative of three independent experiments (A-E). NS, not significant; ND, not detected; *p < 0.05 (Student's *t*-test, error bars represent SD). Please also see Figure S1.

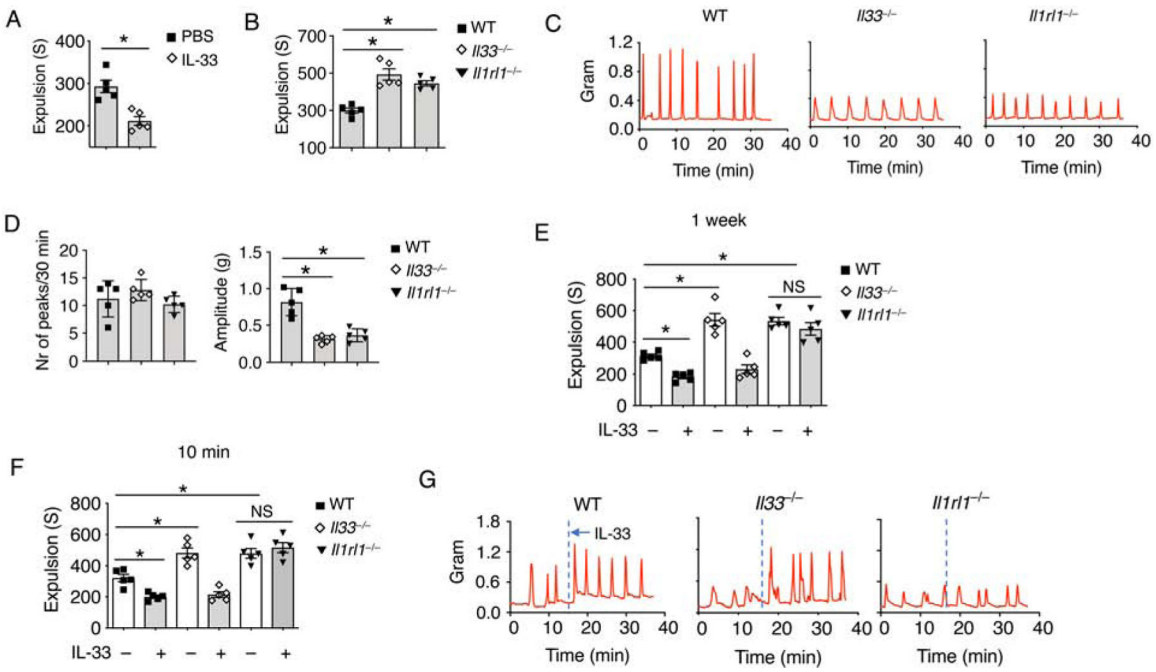

Figure 2. IL-33-ST2 signal regulates gut motility.

(A) WT mice were treated daily with IL-33 or PBS for 7 days. Colonic transit time was assessed by bead expulsion assay.

(B) Colonic transit time was measured by bead expulsion assay in WT, *Il33*$^{-/-}$ and *Il1rl1*$^{-/-}$ mice.

(C) Representative trace and (D) Quantification of colon contraction in WT, *Il33*$^{-/-}$ and *Il1rl1*$^{-/-}$ mice.

(E) WT, *Il33*$^{-/-}$ and *Il1rl1*$^{-/-}$ mice were treated daily with PBS or IL-33 for 7 days. Colonic transit time was assessed by bead expulsion assay at day 8.

(F) WT, *Il33*$^{-/-}$ and *Il1rl1*$^{-/-}$ mice were treated with PBS or IL-33, and waited for 10 minutes. Colonic transit time measured by bead expulsion assay.

(G) Representative trace of IL-33-induced colon contraction in WT, *Il33*$^{-/-}$ and *Il1rl1*$^{-/-}$ mice.

Data are representative of three independent experiments (C, G) or are pooled from two independent experiments (A, B, D-F). NS, not significant; *p < 0.05 (Student's *t*-test, error bars represent SD). Please also see Figure S2.

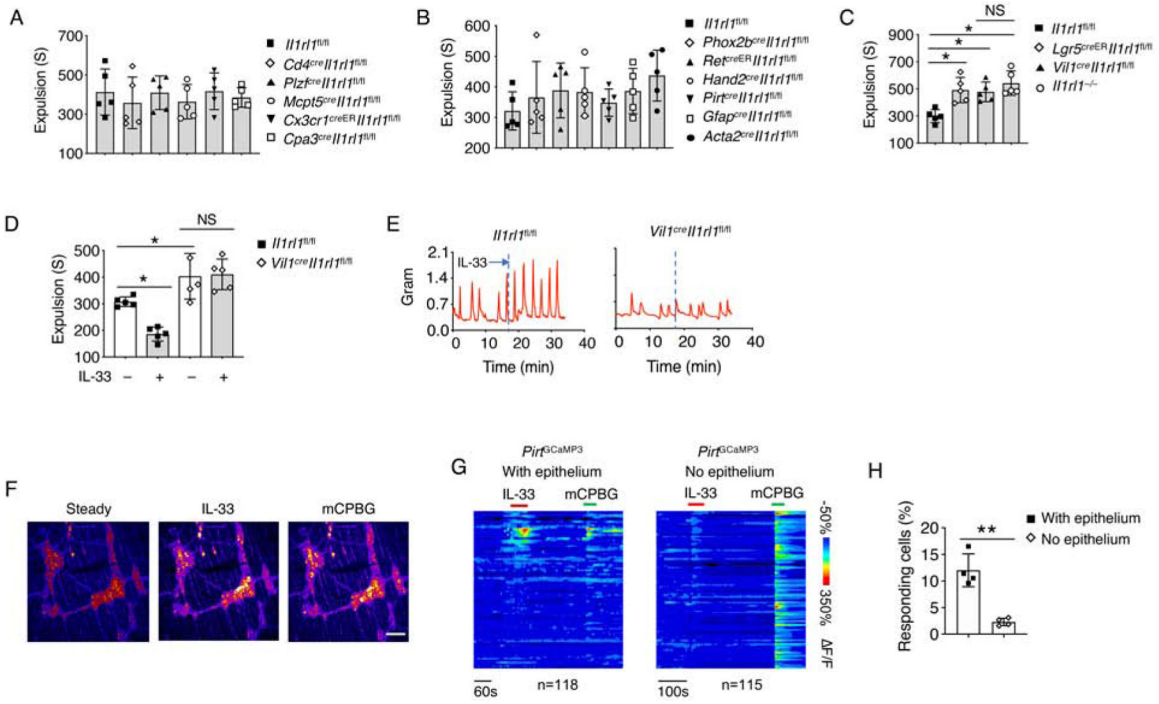

Figure 3. IEC-derived ST2 is required for gut motility.

(A-C) Colonic transit time was assessed by bead expulsion assay in the indicated mouse strains.

(D) *Il1rl1*$^{fl/fl}$ and *Vil1*^{cre}*Il1rl1*$^{fl/fl}$ mice were treated with PBS or IL-33, and waited for 10 minutes. Colonic transit time was assessed by bead expulsion assay.

(E) Representative trace of IL-33-induced colon contraction in *Il1rl1*$^{fl/fl}$ and *Vil1*^{cre}*Il1rl1*$^{fl/fl}$ mice.

(F) GCaMP3 fluorescence signal of neurons on the myenteric plexus of *Pirt*^{GCaMP3} mice treated with IL-33 and mCPBG ($5HT_3R$ agonist).

(G) Time-resolved responses (ΔF/F, color scale) of neurons (one neuron per row) and (H) Quantification of IL-33 responding neurons in the myenteric plexus with or without epithelium. mCPBG was used as a positive control.

Data are representative of three independent experiments (E-G) or are pooled from two independent experiments (A-D, H). NS, not significant; *p < 0.05; **p < 0.01 (Student's *t*-test, error bars represent SD). Please also see Figure S3.

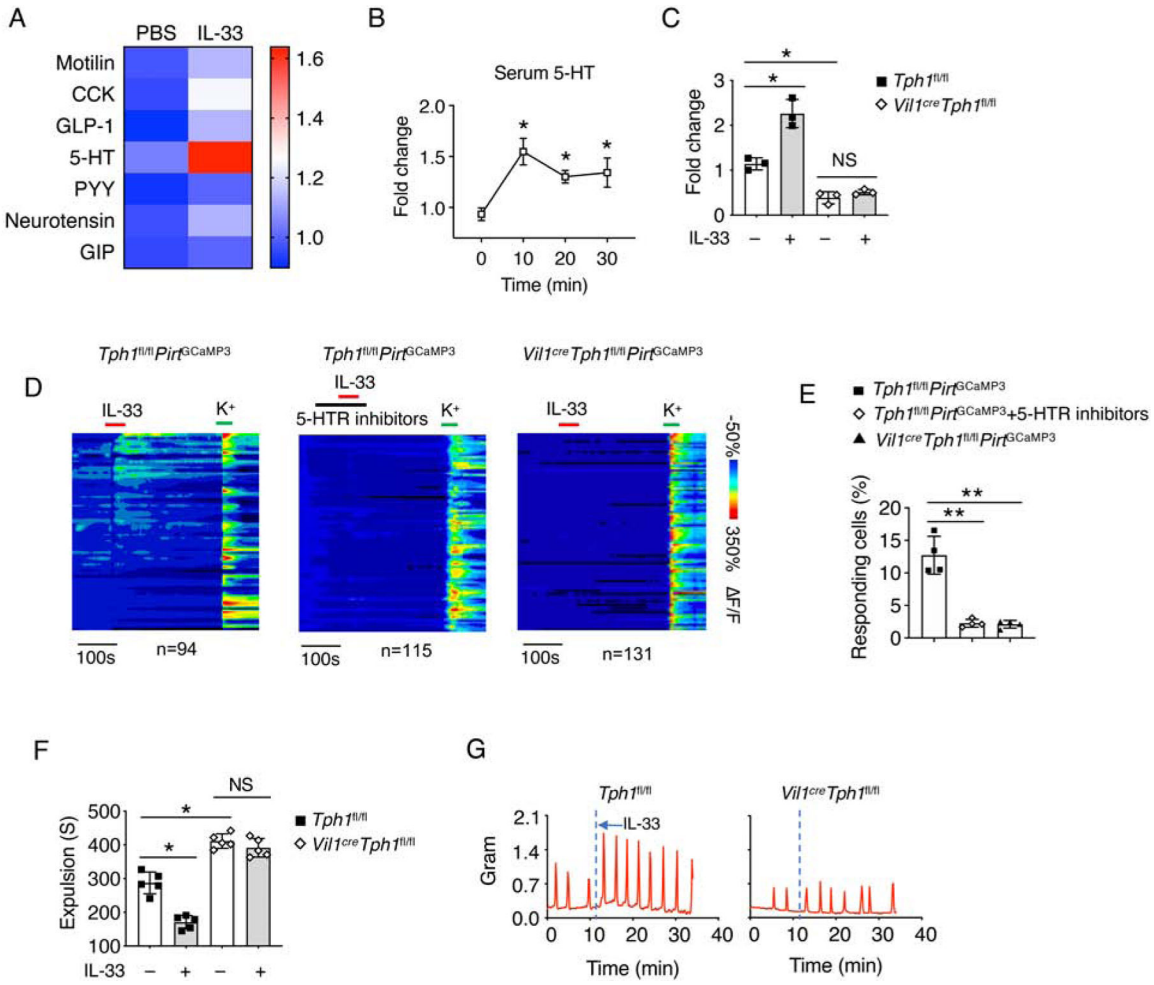

Figure 4. IL-33 induces 5-HT secretion for gut motility.

(A) WT mice were i.p. injected with PBS or IL-33 and waited for 10 minutes. The IEC-derived secretome was assessed from the mice serum.

(B) WT mice were treated with IL-33. Mice serum was collected at the indicated time point, and relative 5-HT amounts were assessed by ELISA.

(C) *Tph1*$^{fl/fl}$ and *Vil1*^{cre}*Tph1*$^{fl/fl}$ mice were treated with PBS or IL-33, and waited for 10 minutes. Mice serum was collected, and relative 5-HT amounts were assessed by ELISA.

(D) Time-resolved responses (ΔF/F, color scale) of neurons (one neuron per row) and (E) Quantification of IL-33 responding neurons in the myenteric plexus treated with the indicated conditions. K^+ was used as a positive control.

(F) *Tph1*$^{fl/fl}$ and *Vil1*^{cre}*Tph1*$^{fl/fl}$ mice were treated with PBS or IL-33, and waited for 10 minutes. Colonic transit time was measured by bead expulsion assay.

(G) Representative trace of IL-33-induced colon contraction in *Tph1*$^{fl/fl}$ and *Vil1*^{cre}*Tph1*$^{fl/fl}$ mice.

Data are representative of three independent experiments (A-D, G) or are pooled from two independent experiments (E, F). NS, not significant; *p < 0.05; **p < 0.01 (Student's *t*-test, error bars represent SD). Please also see Figure S4.

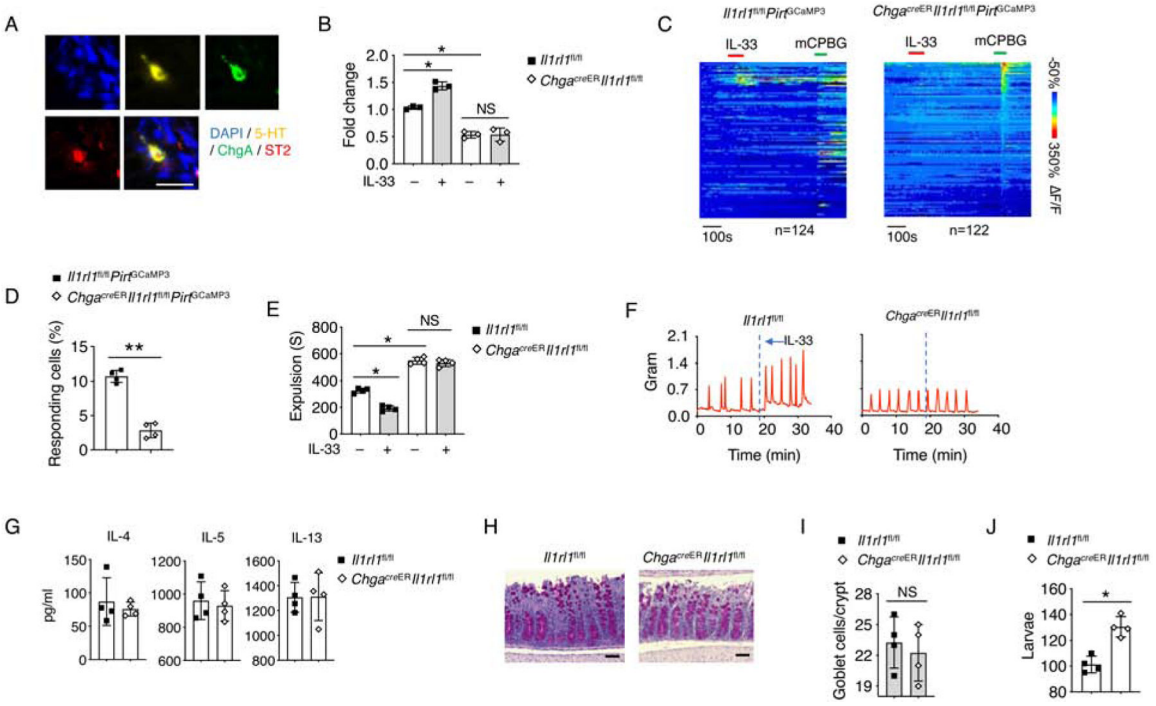

Figure 5. EC cell-derived ST2 responds to IL-33 for 5-HT release.

(A) Representative immunofluorescence staining for 5-HT, chromogranin A (ChgA), ST2 with DAPI in the intestinal tissues of WT mice. Scale bar, 10 μm.

(B) *Il1rl1*$^{fl/fl}$ and *Chga*^{creER}*Il1rl1*$^{fl/fl}$ mice were treated with PBS or IL-33, and waited for 10 minutes. Mice serum was collected, and relative 5-HT amounts were assessed by ELISA

(C) Time-resolved responses (ΔF/F, color scale) of neurons (one neuron per row) and (D) Quantification of IL-33 responding neurons in the myenteric plexus. mCPBG ($5HT_3R$ agonist) was used as a positive control.

(E) *Il1rl1*$^{fl/fl}$ and *Chga*^{creER}*Il1rl1*$^{fl/fl}$ mice were treated with PBS or IL-33, and waited for 10 minutes. Colonic transit time was measured by bead expulsion assay.

(F) Representative trace of IL-33-induced colon contraction in *Il1rl1*$^{fl/fl}$ and *Chga*^{creER}*Il1rl1*$^{fl/fl}$ mice.

(G-J) *T. muris* eggs were inoculated into *Il1rl1*$^{fl/fl}$ and *Chga*^{creER}*Il1rl1*$^{fl/fl}$ mice (pre-treated with tamoxifen) by oral gavage and the mice were sacrificed on day 14 for further testing.

(G) IL-4, IL-5 and IL-13 protein concentrations from mLN were assessed by ELISA.

(H) PAS staining and (I) Quantification of goblet cells per crypt in colonic tissues. Scale bar, 50 μm.

(J) Quantification of larvae in the colonic tissues.

Data are representative of two independent experiments (A-C, F-J) or are pooled from two independent experiments (D, E). NS, not significant; *$p < 0.05$; **$p < 0.01$ (Student's *t*-test, error bars represent SD). Please also see Figure S5.

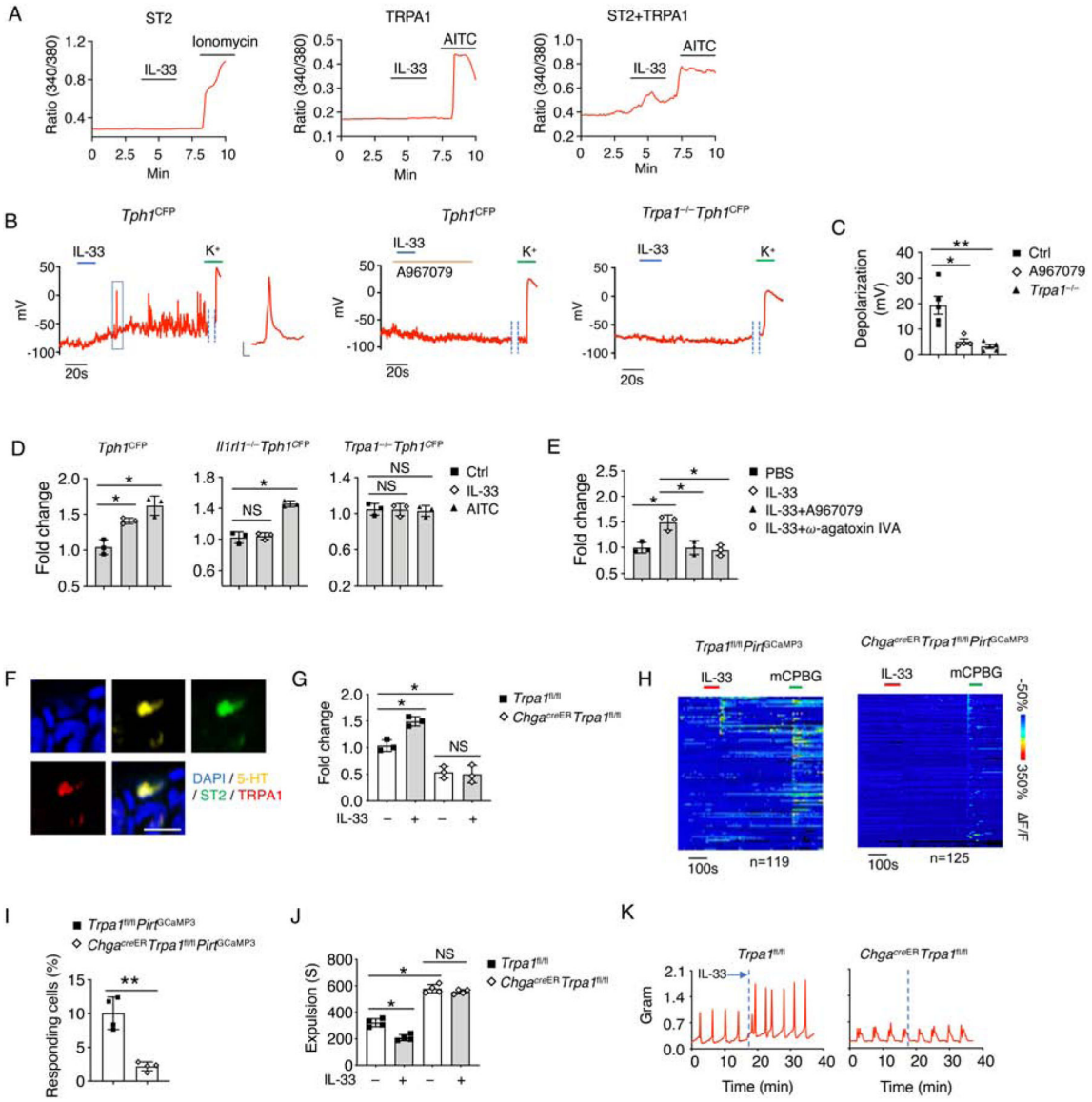

Figure 6. TRPA1 is required for IL-33-mediated 5-HT release.

(A) Representative time-lapse Ca^{2+} imaging traces of IL-33-induced $[Ca^{2+}]_i$ response in NIH 3T3 cells overexpressed with ST2 alone; or with TRPA1 alone; or with both ST2 and TRPA1. Ionomycin and AITC were used as positive controls.

(B) Representative trace and (C) Quantification of IL-33-induced action potentials were recorded by whole-cell patch-clamp from isolated EC cells of *Tph1*^{CFP} mice with or without A967079 (TRPA1 antagonist), or isolated EC cells of *Trpa1*$^{-/-}$*Tph1*^{CFP} mice. K^+ was used as a positive control. Inset: representative action potential. Scale bar, 20 mV, 10 ms.

(D) Relative 5-HT amounts in the cultured supernatant from EC cell-enriched intestinal organoids treated with PBS, IL-33 or AITC (TRPA1 agonist) for 8 hours were assessed by ELISA.

(E) Relative 5-HT amounts in the cultured supernatant from EC cell-enriched intestinal organoids treated with the indicated conditions for 8 hours derived from *Tph1*^{CFP} mice were assessed by ELISA. A967079 (TRPA1 antagonist). ω-agatoxin IVA (Ca^{2+} channel blocker).
(F) Representative immunofluorescence staining for 5-HT, ST2, TRPA1 and DAPI in the colonic tissues of WT mice. Scale bar, 10 μm.
(G) *Trpa1*$^{fl/fl}$ and *Chga*^{creER}*Trpa1*$^{fl/fl}$ mice were treated with PBS or IL-33, and waited for 10 minutes. Mice serum was collected, and relative 5-HT amounts were assessed by ELISA.
(H) Time-resolved responses (ΔF/F, color scale) of neurons (one neuron per row) and (I) Quantification of *Trpa1*$^{fl/fl}$*Prit*^{GCaMP3} and *Chga*^{creER}*Trpa1*$^{fl/fl}$*Prit*^{GCaMP3} mice that were treated with the indicated conditions. mCPBG ($5HT_3R$ agonist) was used as a positive control.
(J) *Trpa1*$^{fl/fl}$ and *Chga*^{creER}*Trpa1*$^{fl/fl}$ mice were treated with PBS or IL-33, and waited for 10 minutes. Colonic transit time was measured by bead expulsion assay.
(K) Representative trace of IL-33-induced colon contraction in *Trpa1*$^{fl/fl}$ and *Chga*^{creER}*Trpa1*$^{fl/fl}$ mice.
Data are representative of three independent experiments (A, B, D-H, J, K) or are pooled from two independent experiments (C, I). NS, not significant; *p < 0.05; **p < 0.01 (Student's *t*-test, error bars represent SD). Please also see Figure S6.

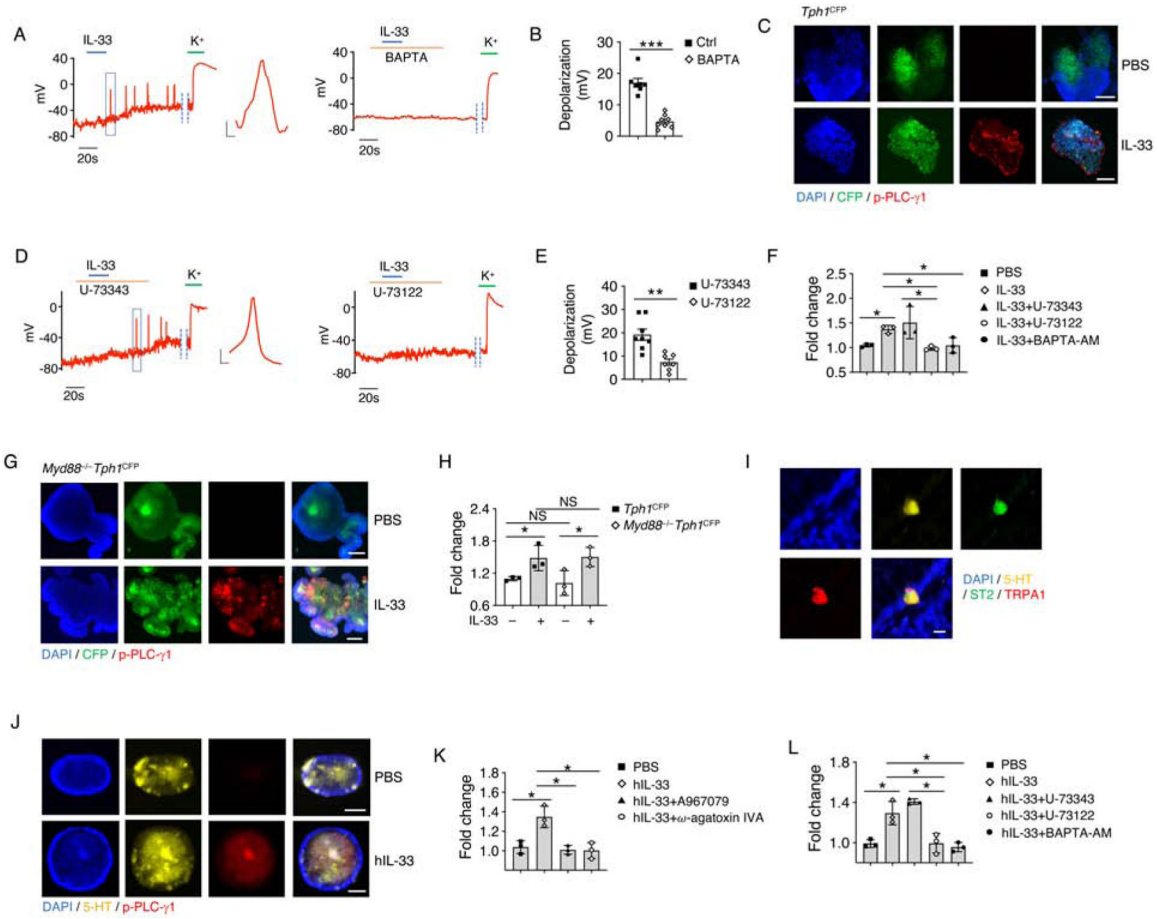

Figure 7. IL-33 induces PLC-γ1 activation for 5-HT release in EC cells.

(A) Representative trace and (B) Quantification IL-33-induced action potentials were recorded by whole-cell patch-clamp from isolated EC cells of *Tph1*^{CFP} mice with or without BAPTA. K^+ was used as a positive control. Inset: representative action potential. Scale bar, 20 mV, 10 ms. BAPTA (calcium chelator, cell-impermeant).

(C) *Tph1*^{CFP} EC-enriched intestinal organoids were treated with PBS or IL-33 for 10 minutes and fixed. Representative immunofluorescence staining for TPH1-CFP, p-PLC-γ1 and DAPI. Scale bar, 100 μm.

(D) Representative trace and (E) Quantification of IL-33-induced action potentials were recorded by whole-cell patch-clamp in isolated EC cells from *Tph1*^{CFP} mice treated with U-73343 (inactive analog of PLC-γ1 inhibitor U-73122) or U-73122. Inset: representative action potential; K^+ was used as a positive control. Scale bar, 20 mV, 10 ms.

(F) Relative 5-HT amounts in the cultured supernatant from EC-enriched intestinal organoids treated with the indicated conditions for 8 hours derived from *Tph1*^{CFP} mice were assessed by ELISA. BAPTA-AM (calcium chelator, cell-permeant).

(G) *Myd88*$^{-/-}$ *Tph1*^{CFP} EC-enriched intestinal organoids were treated with PBS or IL-33 for 10 minutes and fixed. Representative immunofluorescence staining for TPH1-CFP, p-PLC-γ1 and DAPI. Scale bar, 100 μm.

(H) Relative 5-HT amounts in the cultured supernatant from EC-enriched intestinal organoids derived from *Tph1*^{CFP} and *Myd88*$^{-/-}$ *Tph1*^{CFP} mice treated with PBS or IL-33 for 8 hours were assessed by ELISA.

(I) Representative immunofluorescence staining for 5-HT, ST2, TRPA1 and DAPI in the healthy human intestinal tissues. Scale bar, 10 μm.

(J) Human EC cell-enriched intestinal organoids were treated with PBS or IL-33 for 10 minutes and fixed. Representative immunofluorescence staining for 5-HT, p-PLC-γ1 with DAPI. Scale bar, 100 μm.

(K-L) The human EC cell-enriched intestinal organoids were treated with the indicated conditions for 8 hours. Relative 5-HT amounts in the cultured supernatant were assessed by ELISA.

Data are representative of three independent experiments (A, C, D, F-L) or are pooled from two independent experiments (B, E). NS, not significant; *p < 0.05; **p < 0.01; ***p < 0.001 (Student's *t*-test, error bars represent SD). Please also see Figure S7.

Key Resources Table

Reagent or resource	Source	Identifier
Antibodies		
Anti-Tublin-βIII	Biolegend	801202
Anti-GFP	Abcam	ab290
Anti-ChgA	Abcam	ab15160
Anti-ST2 for histology	Proteintech	60112–1-Ig
Anti-5-HT	Abcam	ab66047
Brilliant Violet 421™ anti-ST2	Biolegend	145309
APC anti-EpCam	Biolegend	118214
Anti-TRPA1	Novus Biologicals	NB110–40763
Anti-Phospho-PLCγ1 (Tyr783)	Cell signaling	2821
Anti-PLCγ1	Cell signaling	5690
Anti-β-actin	Sigma	A5441
Helminth Strain		
Trichuris muris	USDA, Joseph Urban Jr	N/A
Chemicals, Peptides, and Recombinant proteins		
Allyl isothiocyanate	Sigma	377430
ω-agatoxin IVA	R&D systems	2799
BAPTA	Sigma	14510
BAPTA-AM	Sigma	A1076
Granisetron	R&D Systems	2903/10
RS 23597–190	R&D Systems	0728/10
Tamoxifen	Sigma	T5648
m-Chlorophenylbiguanide hydrochloride	R&D systems	0440
Isovalerate	Sigma	129542
U73122	Sigma	U6756
U73343	Sigma	U6881
Ionomycin	Sigma	I9657
A967079	Sigma	SML0085
Y-27632	Sigma	Y0503
Sylgard-184	Dow Corning Corp	4019862
Vancomycin	Sigma	V2002
Neomycin	Sigma	N1876
Metronidazole	Sigma	M3761
Ampicillin	Sigma	A9518
Recombinant Mouse IL-33	Biolegend	580506
Recombinant Human IL-33	Biolegend	581804
EDTA (0.5M), PH 8.0	Thermo Fisher Scientific	AM9261

Reagent or resource	Source	Identifier
Collagenase XI	Sigma	C7657
Dnase I	Sigma	10104159001
Dimethyl sulfoxide (DMSO)	Sigma	D8418
DMEM	Thermo Fisher	11965118
IntestiCult™ Organoid Growth Medium (Mouse)	Stemcell technologies	06005
Corning™ Matrigel™ GFR Membrane Matrix	Fisher Scientific	CB-40230C
STEMdiff™ Intestinal Organoid Growth Medium	Stemcell technologies	05145
Essential 8™ Medium	Thermo Fisher	A1517001
DAPT	Sigma	D5942
IWP-2	Sigma	I0536
PD 0325901	Sigma	PZ0162
Fluoromount-G™, with DAPI	Thermo Fisher	00-4959-52
Critical Commercial Assays		
Mouse IL-4 DuoSet ELISA	R&D Systems	DY404–05
Mouse IL-5 DuoSet ELISA	R&D Systems	DY405–05
Mouse IL-13 DuoSet ELISA	R&D Systems	DY413–05
Mouse Motilin (MTL) ELISA Kit	American Research Products, Inc.	KTE70927
Mouse CCK EIA	RayBiotech	EIAM-CCK-1
Mouse PYY EIA	RayBiotech	EIAM-PYY-1
Mouse GLP-1 EIA	RayBiotech	EIAM-GLP1–1
Mouse Neurotensin EIA	RayBiotech	EIAM-NT-1
Mouse GIP EIA	RayBiotech	EIAM-GIP-1
Serotonin ELISA Kit	Abnova	KA1894
iScript RT Supermix for RT-qPCR	Biorad	1708841
STEMdiff™ Intestinal Organoid Kit	Stemcell technologies	05140
Experimental Models: Organisms/Strains		
Mouse: C57BL6/J	Jackson Laboratory	000664
Mouse: *Il4*$^{-/-}$*Il13*$^{-/-}$	Taconic	Line 242
Mouse: *Il33*$^{-/-}$	S. Nakae	N/A
Mouse: *Il1rl1*$^{-/-}$	G. Trinchieri	N/A
Mouse: *Il1rl1*^{flox}	KOMP	N/A
Mouse: *Cd4*^{Cre}	Jackson Laboratory	022071
Mouse: *Plzf*^{Cre}	Jackson Laboratory	024529
Mouse: *Mcpt5*^{Cre}	A. Roers	N/A
Mouse: *Cx3Cr1*^{CreER}	Jackson Laboratory	021160
Mouse: *Cpa3*^{Cre}	Jackson Laboratory	026828
Mouse: *Phox2b*^{Cre}	Jackson Laboratory	016223
Mouse: *Ret*^{CreER}	D. Ginty	N/A
Mouse: *Hand2*^{Cre}	D. Clouthier	N/A

Reagent or resource	Source	Identifier
Mouse: *Pirt*^{Cre}	X. Dong	N/A
Mouse: *Gfap*^{Cre}	Jackson Laboratory	012886
Mouse: *Acta2*^{Cre}	Jackson Laboratory	029925
Mouse: *Lgr5*^{CreER}	Jackson Laboratory	008875
Mouse: *Vil1*^{Cre}	Jackson Laboratory	021504
Mouse: *Pirt*G^{CaMP3}	X. Dong	N/A
Mouse: *Tph1*^{flox}	G. Karsenty	N/A
Mouse: *Chga*$^{CreER-GFP}$	EMMA	09574
Mouse: *Tph1*^{CFP}	A. Leiter	N/A
Mouse: *Trpa1*$^{-/-}$	Jackson Laboratory	006401
Mouse: *Trpa1*^{flox}	C. Stucky	N/A
Mouse: Myd88$^{-/-}$	Jackson Laboratory	009088
Mouse: *Myd88*^{flox}	Jackson Laboratory	008888
Mouse: *Stat6*$^{-/-}$	Jackson Laboratory	005977
Mouse: *Rag2*$^{-/-}$ *Il2rg*$^{-/-}$	Taconic	Line 111
Experimental Models: Cell lines		
NIH 3T3	ATCC	CRL-1658™
Recombinant DNA		
Plasmid: mouse ST2	Sino Biological	HG10105-M
Plasmid: mouse TRPA1	Genscript	OMu22951
Plasmid: mouse TRPC4	Genscript	OMu31798
Plasmid: mouse Olfr558	(Saito et al., 2009)	Addgene: 22333
Oligonucleotides		
Il4 - forward 5' GGTCTCAACCCCCAGCTAGT	IDT	N/A
Il4 - reverse 5' GCCGATGATCTCTCTCAAGTGAT	IDT	N/A
Il5 - forward 5' CTCTGTTGACAAGCAATGAGACG	IDT	N/A
Il5 - reverse 5' TCTTCAGTATGTCTAGCCCCTG	IDT	N/A
Il13 - forward 5' CCTGGCTCTTGCTTGCCTT	IDT	N/A
Il13 - reverse 5' GGTCTTGTGTGATGTTGCTCA	IDT	N/A
Tph1 - forward 5' ATGGATCCGAACTTGACGCC	IDT	N/A
Tph1 - reverse 5' GGGTCCCCATGTTTGTAGTTC	IDT	N/A
Slc6a4 - forward 5' GCGACGTGAAGGAAATGCTGG	IDT	N/A
Slc6a4 - reverse 5' ATAGGGATGCAGATGACAGACG	IDT	N/A
Slc18a1 - forward 5' TCTCTGGCACCTATGCCCT	IDT	N/A

Reagent or resource	Source	Identifier
Slc18a1 - reverse 5' TGCCCACAAATTCATACATCACA	IDT	N/A
Ddc - forward 5' TAGCTGACTATCTGGATGGCAT	IDT	N/A
Ddc - reverse 5' GTCCTCGTATGTTTCTGGCTC	IDT	N/A
Maoa - forward 5' GCCCAGTATCACAGGCCAC	IDT	N/A
Maoa - reverse 5' GTCCCACATAAGCTCCACCA	IDT	N/A
Maob - forward 5' ATGAGCAACAAAAGCGATGTGA	IDT	N/A
Maob - reverse 5' TCCTAATTGTGTAAGTCCTGCCT	IDT	N/A
Actb - forward 5' GGCTGTATTCCCCTCCATCG	IDT	N/A
Actb - reverse 5' CCAGTTGGTAACAATGCCATGT	IDT	N/A
Software and Algorithms		
GraphPad Prism version 8 for MacOS	Graphpad Software	https://www.graphpad.com
Fiji	ImageJ	https://imagej.net/Welcome
Microsoft Excel for MacOS	Microsoft	https://products.office.com/en-us/excel
Zen	Zeiss	https://www.zeiss.com/microscopy/us/products/microscope-software/zen.html
Imaris (v. 8.4)	Bitplane	http://www.bitplane.com/imaris/imaris
pClamp 10.6	Molecular Devices	https://www.moleculardevices.com/products/axon-patch-clamp-system/acauisition-and-analysis-software/pclamp-software-suite#gref
LabChart	AD instruments	https://www.adinstruments.com/products/labchart

Reagent or resource	Source	Identifier
NIS-elements	Nikon	https://www.microscope.healthcare.nikon.com/products/software/nis-elements
FlowJo	TreeStar	https://www.flowjo.com/